HHS Public Access

Author manuscript

Immunity. Author manuscript; available in PMC 2019 December 18.

Published in final edited form as:

Immunity. 2018 December 18; 49(6): 1077–1089.e5. doi:10.1016/j.immuni.2018.10.014.

Microbiota-induced TNF-like ligand 1A drives group 3 innate lymphoid cell-mediated barrier protection and intestinal T cell activation during colitis

Jim G. Castellanos[1], **Viola Woo**[1], **Monica Viladomiu**[1], **Gregory Putzel**[1], **Svetlana Lima**[1], **Gretchen E. Diehl**[2], **Andrew Marderstein**[1], **Jorge Gandara**[1], **Alexendar R. Perez**[1], **David R. Withers**[3], **Stephan R. Targan**[4], **David Q. Shih**[4], **Ellen J. Scherl**[5], and **Randy S. Longman**[1,5,*]

[1]Jill Roberts Institute for Research in IBD, Weill Cornell Medicine, New York, NY, 10021, USA

[2]Alkek Center for Metagenomics and Microbiome Research, Baylor College of Medicine, Houston, TX, 77030, USA

[3]Institute of Immunology and Immunotherapy, College of Medical and Dental Sciences, University of Birmingham, Birmingham, UK

[4]F. Widjaja Foundation, Inflammatory Bowel and Immunology Research Institute, Cedars-Sinai Medical Center, Los Angeles, California, 90048, USA

[5]Jill Roberts Center for IBD, Weill Cornell Medicine, New York, NY, 10021, USA

SUMMARY

Inflammatory bowel disease (IBD) results from a dysregulated interaction between the microbiota and a genetically susceptible host. Genetic studies have linked *TNFSF15* polymorphisms and its protein TNF-like ligand 1A (TL1A) with IBD, but the functional role of TL1A is not known. Here, we found that adherent IBD-associated microbiota induced TL1A release from $CX3CR1^{+}$ mononuclear phagocytes (MNPs). Using cell- specific genetic deletion models, we identified an essential role for $CX3CR1^{+}$MNP- derived TL1A in driving group 3 innate lymphoid cell (ILC3) production of interleukin 22 and mucosal healing during acute colitis. In contrast to this protective role in acute colitis, TL1A-dependent expression of co-stimulatory molecule OX40L in $MHCII^{+}$ ILC3s during colitis led to co-stimulation of antigen-specific T cells that was required for chronic T cell colitis. These results identify a role for ILC3s in activating intestinal T cells and reveal a central role for TL1A in promoting ILC3 barrier immunity during colitis.

*Corresponding author: Lead Contact: ral2006@med.cornell.edu.

Author contributions: Conceptualization and Methodology, J.G.C., D.W., G.E.D., S.R.T., D.Q.S. and R.S.L; Investigation, J.G.C, V.W., M.V., R.S.L.; Formal Analysis, J.G.C., V.W., M.V., G.P., G.E.D., S.L., A.M., A.R.P; Resources, S.R.T, D.Q.S., E.J.S., D.W., R.S.L.; Data Curation, G.P., S.L., A.M., J.G., A.R.P; Writing-Original Draft, J.G.C. and R.S.L.; Writing-Review and Editing, J.G.C and R.S.L. Visualization, J.G.C and R.S.L. Supervision, R.S.L.; Funding Acquisition, G.E.D., S.R.T., D.Q.S., R.S.L.

Declaration of Interests: S.R.T. is co-founder and consultant to Precision IBD Inc. G.E.D. and R.S.L. have submitted Patent Application No. 14/797,588.

Data and Software Availability

RNA seq data have been deposited in GEO repository accession GSE120723.

One Sentence Summary:

Microbial-induced TL1A regulates the innate and adaptive functions of ILC3 in colitis

eTOC/In Brief

Inflammatory bowel disease (IBD) results from a dysregulated interaction between the microbiota and a genetically susceptible host. Castellanos et al. show a protective role for microbial induction of the IBD-linked protein TL1A in promoting ILC3 barrier immunity and uncover a pathogenic role for TL1A-induced expression of OX40L on ILC3s in driving chronic T cell colitis.

Abstract

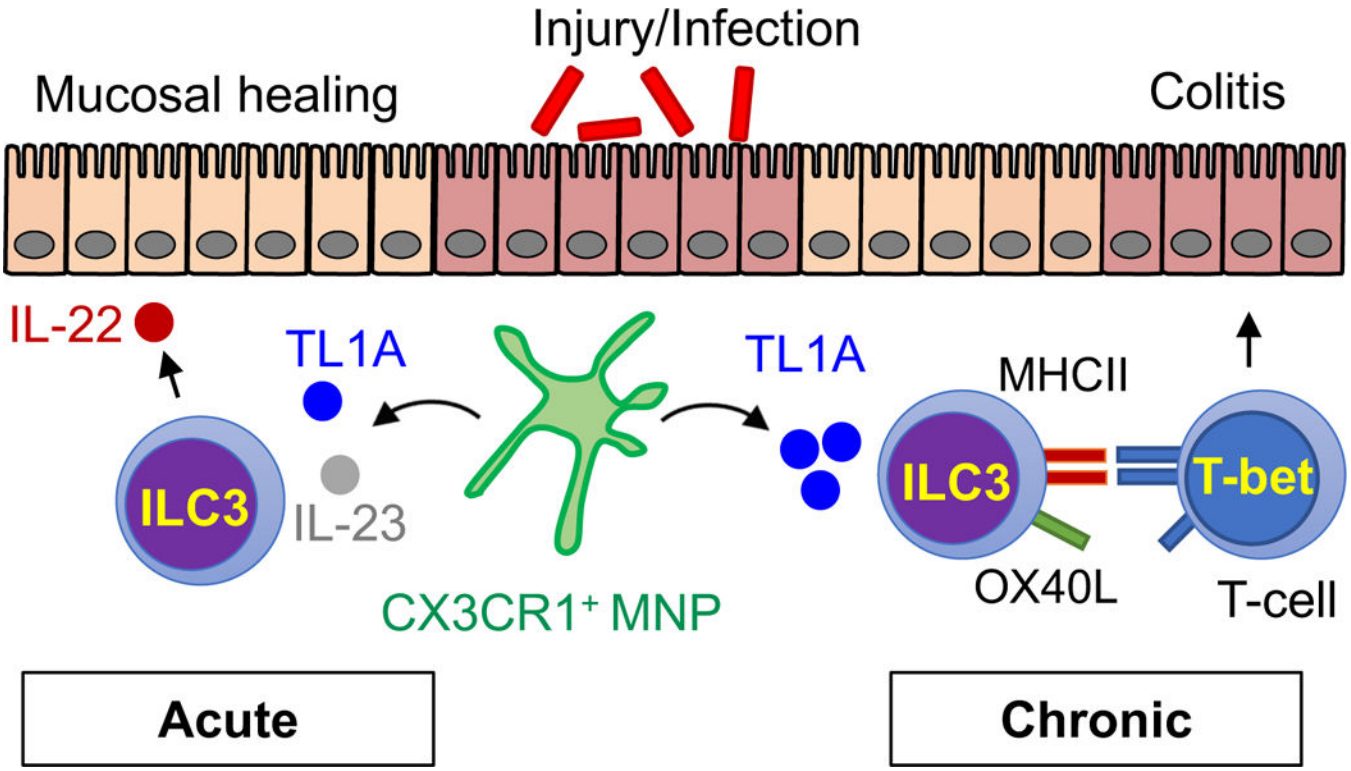

Keywords

Inflammatory bowel disease; Crohn's disease; CX_3CR1^+ mononuclear phagocytes; Innate Lymphoid Cell; TL1A

INTRODUCTION

Inflammatory bowel disease (IBD) affects over 4 million people worldwide, causing significant morbidity among patients (Kaplan, 2015). IBD pathogenesis is thought to be multifactorial, with both intestinal dysbiosis and genetic components underlying disease pathogenesis. Characteristic alterations in the IBD-associated microbiome exist, with marked contraction of intestinal microbial diversity a hallmark of IBD (Gevers et al., 2014).

Genetic studies have identified over 200 genes linked with IBD susceptibility (McGovern et al., 2015), but our functional understanding of how these genes contribute to intestinal homeostasis and IBD pathophysiology is incomplete, limiting the potential for diagnostic and therapeutic intervention.

Genome-wide association studies (GWAS) in IBD have revealed strong associations of genetic variants in *TNFSF15* with Crohn's disease, highlighting a central role for its protein, TNF-like ligand 1A (TL1A), in mucosal immunity (Siakavellas and Bamias, 2015). Variants in *TNFSF15* have been linked to the pathogenesis of several autoimmune diseases—including psoriasis, rheumatoid arthritis, and multiple sclerosis—implicating a broader role for TL1A in human inflammatory diseases. In IBD, *TNFSF15* variants confer higher risk for more aggressive, penetrating, fibrostenotic, and perianal disease complications (Tung et al., 2014; Yang et al., 2014), but the mechanistic impact of TL1A remains controversial. While early studies showed a pathogenic role for TL1A in driving inflammatory T cell response (Prehn et al., 2004; Zheng et al., 2013), more recent reports in acute colitis models revealed a protective role for TL1A (Jia et al., 2016). Genetic models are needed to understand the cellular mechanisms and potential therapeutic targetability of this IBD-linked pathway in intestinal inflammation.

Group 3 innate lymphoid cells (ILC3s) are an emerging class of innate lymphocytes that play a critical role in regulating mucosal homeostasis. In response to environmental triggers, in particular the cytokines IL-23 and IL-1β, ILC3s produce robust amounts of IL-22 and play an important role in maintaining intestinal barrier integrity and promoting mucosal healing—a major clinical endpoint in IBD (Longman et al., 2014). Co-localization of ILC3s with $CX3CR1^+$ mononuclear phagocytes (MNPs) in the lamina propria enables rapid regulation of ILC3 effector cytokines to reinforce barrier immunity and mucosal healing (Satoh-Takayama et al., 2014). Both mouse and human ILC3s express Death Receptor 3 (DR3), the monogamous receptor for TL1A, on its surface, with TL1A stimulation promoting ILC3 proliferation (Ahn et al., 2015) and cytokine production *in vitro* (Longman et al., 2014); however, the role for TL1A in regulating ILC3 function in intestinal homeostasis, and its potential contribution to IBD pathophysiology, remains unknown.

Here, we generated mouse models with selective deletion of TL1A and its receptor DR3 to evaluate the role of this critical IBD-linked genetic pathway in regulating mucosal immunity. Our data revealed a central role for $CX3CR1^+$ MNP-derived TL1A, which is induced by adherent IBD-associated microbiota, in regulating ILC3 production of IL-22 and mucosal healing in acute colitis. In addition to regulating cytokine production, TL1A induced OX40 ligand (OX40L) expression on colonic ILC3 in mouse and human colitis. OX40L expression on $MHCII^+$ ILC3s supported antigen-specific T proliferation *in vitro* and pathogenic T helper 1 (Th1) cell expansion in chronic colitis models. Our findings reveal a central role for IBD-linked TL1A in regulating ILC3 barrier immunity and uncover a mechanistic role for TL1A-induced expression of the costimulatory molecule OX40L on $MHCII^+$ ILC3s in regulating colonic T cells.

RESULTS

Mononuclear phagocyte TL1A promotes barrier protection during acute colitis

CX_3CR1^+ MNPs play a central role in coordinating the mucosal immune response during colitis (Kim et al., 2018; Longman et al., 2014; Panea et al., 2015; Satoh- Takayama et al., 2014). Recent studies have reported increased TL1A protein in the colonic tissue of both mouse and humans during active colitis (Bamias et al., 2013) (Zheng et al., 2013). To evaluate the cellular source of TL1A in the human intestine, we performed TL1A staining of lamina propria mononuclear cells (LPMCs). TL1A expression was significantly higher on $CD14^+HLA\text{-}DR^{hi}$ intestinal MNPs compared to lymphocytes (Fig. 1A). To evaluate the impact of colitis on MNP expression of TL1A, we performed flow cytometry on lamina propria mononuclear cells from endoscopic biopsies from healthy controls (N=8) or individuals with ileocolonic Crohn's disease (CD, inactive N=3, active N=8) (Fig. 1B, S1A). MNPs from CD patients with active inflammation showed significantly higher surface expression of TL1A (Fig. 1B). Consistent with these data from human CD, selective depletion of $CX3CR1^+$ MNP using mice harboring a diphtheria toxin receptor (DTR) insertion into the *Cx3cr1* locus ($Cx3cr1^{DTR}$) (Longman et al., 2014) following diphtheria toxin injection significantly reduced TL1A expression in the intestinal lamina propria (Fig. 1C). These data demonstrate that $CX3CR1^+$ MNPs are a primary source of intestinal TL1A, which is significantly upregulated during active Crohn's disease.

To evaluate the potential physiological role for MNP-derived TL1A in colitis, we generated mice with a TL1A conditional deletion allele with *lox*P-flanked *Tnfsf15* (*Tnfsf15*$^{flox/flox}$) and crossed to *Itgax-cre* mice to specifically delete TL1A in cells expressing CD11c (*Tnfsf15*$^{flox/flox}$*Itgax-cre,* subsequently referred to as $TL1A^{\Delta CD11c}$). TL1A mRNA expression in lamina propria $CD11c^+$ cells was used to confirm deletion (Fig. S1B). $TL1A^{\Delta CD11c}$ mice exposed *ad libitum* to 2% dextran sodium sulfate (DSS) for seven days lost significantly more weight than their littermate controls (Fig. 1D). To specifically test the role for $CX3CR1^+$ MNP-derived TL1A, we crossed $Tnfsf15^{flox/flox}$ mice with mice expressing a tamoxifen-inducible Cre recombinase under control of the *Cxc3cr1* promoter (*Tnfsf15*$^{flox/flox}$*Cx3cr1-creER,* subsequently referred to as $TL1A^{\Delta CX3CR1}$). Transcriptional analysis validated that $TL1A^{\Delta CX3CR1}$ mice selectively lacked TL1A expression on $CD11C^+MHCII^+CD11b^+$ MNPs following induction with tamoxifen (Fig. S1C). To examine a role for $CX3CR1^+$ MNP-derived TL1A *in vivo,* $TL1A^{\Delta CX3CR1}$ and their littermate controls were exposed to 2% DSS for seven days. $TL1A^{\Delta CX3CR1}$ mice lost significantly more weight than their littermate controls and had increased histopathological damage (Fig. 1E, F).

Previous studies have demonstrated that TL1A can affect both T cell and innate lymphoid cell function (Richard et al., 2015). To evaluate the impact of MNP-specific TL1A deletion in regulating lymphocyte effector function during colitis, flow cytometry was performed on LPMCs. Although no differences were seen in T cell subsets or cytokine production (Fig. 1G, S1D), there was a statistically significant reduction in IL- 22 production by ILC3s in TL1A deficient mice (Fig. 1H,S1E). There were no differences in total ILC3 numbers in the colon (Fig. S1F) or in ILC3 production of IL-17 or IFNγ. These models illustrate a central role for MNP-derived TL1A in regulating the innate response to acute colitis.

Adherent CD-associated microbiota induce CX3CR1^{+} MNP-derived TL1A

CX3CR1^{+} MNPs are uniquely positioned at the intestinal barrier to sample luminal microbes and respond to microbial products through toll like receptor signaling (Diehl et al., 2013). Given the ability of bacterial signals to induce TL1A mRNA in human antigen-presenting cells (Shih et al., 2009), we evaluated the effect of MyD88- deficiency on TL1A expression in gut MNPs. MNPs from mice with MyD88-deletion showed a significant reduction in MNP TL1A expression (Fig. 2A). Although CX3CR1 promotes direct microbial sampling via transepithelial dendrites (Niess et al., 2005), CX3CR1-deletion did not affect TL1A expression. To test the role for microbial regulation of TL1A *in vivo,* we compared TL1A expression in germ-free mice and specific pathogen free (SPF) mice. Flow cytometric analysis of TL1A expression in CD11c^{+} MHCII^{+} CD11b^{+} MNPs showed that germ-free mice had a significant reduction in intestinal TL1A protein expression compared to SPF mice (Fig. 2B). Previous studies have reported that microbial adherence to the intestinal epithelial surface may play a critical role in regulating immune responses in the lamina propria. Segmented filamentous bacteria (SFB), for example, adheres tightly to the ileal mucosa and induces Th17 and ILC3 effector function (Ivanov et al., 2009; Sano et al., 2015). Given the importance of CX3CR1^{+} MNP in regulating Th17 and ILC3 effector functions (Longman et al., 2014; Panea et al., 2015), we sought to examine the role for SFB in TL1A regulation. Lamina propria MNPs from germ-free and gnotobiotic mice colonized with SFB were analyzed for TL1A expression (Fig. 2C). SFB mono-colonized mice had significantly higher intestinal TL1A mRNA compared to germ-free mice. To further test if this induction of TL1A was selective for adherent bacteria, we used Adherent-invasive *E.coli* (AIEC) strain 2A and a non-adherent *E. coli* control strain T75 derived from patients with Crohn's disease (Viladomiu et al., 2017). At 5 days following colonization, AIEC strain 2A, but not T75, induced TL1A mRNA in the colonic lamina propria (Fig. 2C). To evaluate the role for microbial regulation of TL1A in SPF mice, we assessed TL1A protein expression using antibiotic-treated *Cx$_3$cr1*$^{GFP/WT}$ mice. Flow cytometric analysis of TL1A protein in CX3CR1^{+} MNPs from antibiotic treated mice showed a significant reduction in intestinal TL1A compared to SPF mice (Fig. 2D). The reduction in MNP expression of TL1A protein induced by antibiotics could be restored by colonization with AIEC 2A (Fig. 2E). Previous studies have reported that CX3CR1^{+} MNP increase cytokine production during colitis (Zigmond et al., 2012). To test whether colitis altered CX3CR1^{+} MNP TL1A, mice were exposed to DSS and TL1A mRNA levels were evaluated in sort-purified CX3CR1^{+} MNP. Barrier disruption with DSS induced increased TL1A mRNA expression in SPF mice, which was further enhanced after AIEC 2A colonization (Fig. 2E). Collectively, these data suggest that mucosal-associated microbiota induce MNP TL1A and enhance its production during colitis.

We have previously shown that AIEC can also induce IL-22 production by ILC3s in gnotobiotic mice, leading to reduced mortality in acute DSS colitis (Viladomiu et al., 2017). To test the role for TL1A in AIEC induction of ILC3 IL-22, mice pre-treated with antibiotics were colonized with AIEC. Similar to our findings in the DSS-induced acute colitis model, TL1A$^{\Delta CD11c}$ mice colonized with AIEC showed reduced production of IL-22 compared to littermate controls (Fig. 2F). To test if the protective effects of AIEC are dependent on MNP-derived TL1A, TL1A$^{\Delta CD11c}$ and littermate control mice were pre-treated with broad-

spectrum antibiotics and then colonized with AIEC strain 2A prior to DSS exposure. Colonization with AIEC was sufficient to rescue the more severe weight loss and reduced survival following treatment with antibiotics, and this rescue required MNP-derived TL1A (Fig. 2G). Collectively, these findings reveal a protective link between IBD-associated adherent microbiota and MNP-derived TL1A during acute colitis.

ILC3-specific DR3 deficiency impairs IL-22 production and exacerbates colitis

To evaluate the impact of endogenous TL1A *in vivo* using experimental colitis models, mice deficient for DR3 *(Tnfrsf25*$^{-/-}$*)* were exposed *ad libitum* to 2% DSS. Similar to recent results (Jia et al., 2016), DSS induced more severe acute colitis in mice deficient for DR3, as evidenced by increased weight loss with a protracted recovery (Fig. 3A) and reduced survival (Fig. 3B). Similar to the TL1A deficient mice, analysis of $CD4^+$ T cells in the lamina propria did not reveal significant differences in $CD4^+Foxp3^+$ T regulatory (Treg) or IL-17-producing $ROR\gamma t^+$ T helper 17 (Th17) cells during acute colitis (Fig. S2A, B). Although overexpression of TL1A can alter ILC2 function (Meylan et al., 2014), we observed no effect of DR3 deletion on IL-13 production by ILC2 cells during acute colitis (Fig. S2C). In contrast, Lin^- $ROR\gamma t^+$ ILC3s from the lamina propria showed a significant decrease in IL-22 (Fig. 3C). To evaluate the functional significance of reduced IL-22 production by ILC3 during colitis, we injected DR3-deficient mice with recombinant IL-22 following exposure to DSS (Fig. 3D). Treatment with rIL-22 rescued the reduced survival of DR3-deficient mice, suggesting a critical role for ILC3-derived IL- 22 in mediating DR3-dependent mucosal healing.

Other cell types, including $CD4^+$ T cells, can significantly contribute to IL-22 production (Basu et al., 2012). To specifically test the importance of ILC3-intrinsic DR3 signaling in IL-22 production and intestinal barrier immunity, we crossed mice with a /oxP-flanked *Tnfrsf25 (Tnfrsf25*$^{flox/flox}$*)* to *Rorc-cre* mice on a RAG2-deficient background *(Tnfrsf25*$^{flox/flox}$ *Rorc-cre RAG2*$^{-/-}$ subsequently referred to as $DR3^{\Delta ILC3}$). Transcriptional and flow cytometric analysis revealed that $DR3^{\Delta ILC3}$ mice lacked DR3 expression on ILC3, but not on ILC2, confirming cell type-specific DR3 deletion (Fig. S3A). Absence of DR3 did not change the total number or frequency of ILC3 subsets in the small or large intestines (Fig. S3B).

To evaluate a role for ILC3-intrinsic DR3 in experimental colitis, we exposed $DR3^{\Delta ILC3}$ mice and their littermate controls to *ad libitium* 2% DSS. Phenocopying DR3- deficiency, $DR3^{\Delta ILC3}$ mice lost significantly more weight (Fig. 3E) and had more severe colitis histopathology (Fig. 3F) than their littermate controls. Flow cytometry analysis revealed lower production of IL-22 by ILC3s from $DR3^{\Delta ILC3}$ mice compared to littermate controls (Fig. 3G). Similar to DR3-deficient animals, treatment with rIL-22 rescued the reduced survival of $DR3^{\Delta ILC3}$ (Fig. 3E). IL-22 is critical for inducing intestinal epithelial cell production of antimicrobial peptides (Kinnebrew et al., 2012) and acute phase reactants (Sano et al., 2015). Reduced expression of both *Reg3g* and *Saa1* in intestinal epithelial cells from $DR3^{\Delta ILC3}$ mice (Fig. 3H) demonstrates the functional impact of reduced IL-22 in ILC3-specific deletion of DR3 during colitis.

To test the role for DR3 in infectious colitis, we used the *Citrobacter rodentium* infectious colitis model, which is dependent on ILC3s during the acute response (Sonnenberg et al., 2011). Similar to the response in DSS colitis, $DR3^{\Delta ILC3}$ mice lost significantly more weight and had reduced survival compared to littermate controls (Fig. 3I). Collectively, these experiments demonstrate a key role for cell-intrinsic DR3 in regulating ILC3 production of IL-22 and protection from acute experimental colitis.

TL1A synergizes with IL-23 via p38 MAPK to mediate protection in acute colitis

To investigate the mechanism for TL1A regulation of ILC3-derived IL-22, we sorted Lin^{-} $CD127^{+}$ $IL\text{-}23R^{GFP}$ ILC3s from the small intestinal lamina propria (Fig. S4A) and stimulated *ex vivo* with either recombinant TL1A, IL-23, or TL1A+IL-23. Although both IL-23 and TL1A induce IL-22 transcription (Fig. 4A), concomitant stimulation with both IL-23 and TL1A induced a robust synergistic IL-22 response (Fig. 4A). We confirmed TL1A synergy with IL-23 was DR3-dependent by sorting ILC3s from DR3- deficient mice as well as heterozygous and WT littermate controls (Fig. 4B).

Distinct ILC3 subsets expressing either the natural cytotoxicity receptor NKp46 (called NCR^{+} ILC3) or chemokine receptor 6 (CCR6) (called lymphoid tissue-inducer-like ILC3) share significant functional overlap in the intestine (Melo-Gonzalez and Hepworth, 2017). Surface DR3 expression was equivalent across all ILC3 subsets (Fig. S4B). Additionally, *ex vivo* TL1A stimulation of sorted intestinal ILC3 revealed synergistic induction of IL-22 protein in all subsets (Fig. 4C).

Conventional signaling downstream of DR3 can occur through mitogen-activated protein kinase (MAPK) or NF-κB pathways (Bamias et al., 2013). To evaluate the role for these signaling pathways in mediating TL1A and IL-23 synergistic induction of IL-22, we profiled protein phosphorylation by flow cytometry. Our results revealed significant phosphorylation of IκBα and p38-MAPK but not ERK following TL1A stimulation of sorted intestinal ILC3s (Fig. 4D). To test the dependence on MAPK or NF-κB signaling, we sorted ILC3 and pre-treated with soluble inhibitors prior to *ex vivo* TL1A stimulation. Although the NF-κB inhibitor NBD did not affect IL-22 production, pre-treatment with TAK1 or p38 MAPK inhibitors (5Z-7-Oxozeaenol and SB203580, respectively) completely blocked TL1A and IL-23 synergistic induction of IL-22 (Fig. 4E). No significant increase in STAT3 phosphorylation was detected in ILC3s stimulated with TL1A and IL-23 compared to IL-23 stimulation alone (Fig. S4C), and no transcriptional increase in *Rorc, Ahr, HIFIa,* or *Stat3* was detected in ILC3s stimulated with TL1A to account for the increase in IL-22 (Fig. S4D). In monocyte-derived macrophages, TL1A synergy with muramyl dipeptide requires autocrine IL-1β to induce inflammatory cytokines (Hedl and Abraham, 2014). However, in contrast to this pathway used in macrophages, IL-1R on ILC3 was dispensable for TL1A and IL-23 synergistic induction of IL-22 (Fig. 4F).

To evaluate a physiologic role for IL-23 and TL1A synergy *in vivo,* we generated mice with both DR3- and IL23R-deficiency *($Tnfrsf25^{-/-}Il23r^{GFP/GFP}$).* Mice with both DR3 and IL23R deficiency showed reduced survival following acute DSS-induced colitis compared to mice with a single deficiency of DR3 or IL23R (Fig. 4G). Collectively, these data reveal the

direct synergy of these IBD-linked pathways in regulating ILC3 production of effector cytokines and protection from acute colitis.

TL1A induces OX40L-dependent co-stimulation of CD4+ T cells by MHCII+ ILC3

In contrast to our findings for an essential role for TL1A and DR3 in protection from acute colitis, previous studies have suggested a pathogenic role for TL1A overexpression in IBD (Zheng et al., 2013). To identify potential genes and pathways regulated by TL1A that may account for the pathogenic effects of DR3 in ILC3s during chronic colitis, we performed RNA-seq of TL1A-stimulated intestinal ILC3s. ILC3s were sort-purified from *Il23r*$^{GFP/WT}$ mice and stimulated for 18 hours with or without recombinant TL1A. In addition to induction of *Csf2* and *Il22,* RNA-seq analysis revealed significant induction of the co-stimulatory molecule OX40L following TL1A stimulation (Fig. 5A), which was confirmed by quantitative PCR of its gene *Tnfsf4* (Fig. 5B). Flow cytometric analysis showed induction of surface expression of OX40L in all ILC3 subsets (Fig. 5C). Previous studies have shown that MHCII$^+$ ILC3s lacking surface expression of classical co-stimulatory molecules negatively regulate T cell responses to commensal bacteria (Hepworth et al., 2013). Therefore, to test if TL1A-induced expression of OX40L could promote antigen-specific T cell responses, MHCII$^+$ and MHCII$^-$ ILC3 were sort-purified from *Il23r*$^{GFP/WT}$ mice and co-cultured with CFSE-labeled naïve OT-II CD4$^+$ T cells, which are specific for chicken ovalbumin (OVA) peptide 323–339, in the presence or absence of OVA peptide or recombinant TL1A stimulation. OVA peptide and TL1A stimulation of MHCII$^+$ ILC3 induced multiple rounds of ovalbumin- specific T cell proliferation, similar to the proliferative levels seen in OVA-loaded dendritic cells (Fig. 5D, E). In contrast, no proliferation was seen in co-cultures with MHCII$^-$ ILC3 or DR3-deficient ILC3 (Fig. 5D, E, F, S5A). To evaluate the role of ILC3 0X40L in co-stimulating T cells, ILC3s were cultured with CFSE-labeled naive OT-II CD4$^+$ T cells in the presence of OVA peptide, recombinant TL1A, and α−0X40L blocking antibodies. Blockade of 0X40L, but not ICOSL, completely inhibited *in vitro* proliferation, suggesting a key role for 0X40L co-stimulation in regulating ILC3-driven T cell proliferation (Fig. 5G, S5B). To further test for a role for ILC3 0X40L expression, we generated mice with a conditional deletion of *Tnfsf4* (Cortini et al., 2017) driven by Rorc- Cre recombinase *(Tnfsf4*$^{flox/flox}$ *Rorc-cre* subsequently referred to as 0X40L$^{\Delta Rorc}$) (Fig. S5C). Sorted intestinal ILC3s from mice without 0X40L failed to support 0T-II T cell proliferation following TL1A stimulation *in vitro* (Fig. 5H, S5D). Finally, to determine if 0X40L was functioning as a co-stimulatory signal or acting independently of MHCII, we sorted ILC3s from mice with MHCII-deficient ILC3 *(H2-Ab1*$^{flox/flox}$*Rorc-cre)* (Hepworth et al., 2015) and tested their capacity for supporting 0T-II T cell proliferation *in vitro.* Despite stimulation with TL1A, MHCII-deficient ILC3s were unable to support 0T-II proliferation (Fig. 5I). These experiments revealed a functional role for TL1A in inducing 0X40L co-stimulation of CD4$^+$ T cells by MHCII$^+$ ILC3s.

ILC3 expression of OX40L in colitis regulates pathogenic T cells

To evaluate ILC3 expression of 0X40L *in vivo* during colitis, we performed flow cytometry on lamina propria ILC3s at steady state and following DSS-induced colitis. Although low 0X40L was seen on ILC3s at steady state, colitis induced robust surface expression of 0X40L protein (Fig. 6A). Expression of 0X40L was significantly reduced on the MHCII$^+$

ILC3s from DR3-deficient mice compared to littermate controls, revealing a key role for TL1A in ILC3 expression of OX40L *in vivo* (Fig. 6B). To determine if ILC3s express OX40L during inflammatory bowel disease (IBD), we profiled ILC3 from human intestinal biopsy samples (Fig. 6C, Fig. S6). Lin$^-$ CD127$^+$ c-Kit$^+$ ILC3 from patients with active CD showed significantly higher levels of surface OX40L expression. Collectively, these results reveal TL1A- and colitis-dependent OX40L expression by intestinal ILC3s in mouse and human.

We next sought to evaluate the role for TL1A-induced ILC3 expression of OX40L in regulating intestinal T cell *in vivo.* To test the role for ILC3 expression of OX40L in regulating antigen-specific T cells, we sorted naïve CD45.1$^+$ OT-II cells and adoptively transferred them into *OX40L*$^{\Delta Rorc}$ mice and littermate controls. Mice were exposed to DSS for 5 days (to induce OX40L) and provided ovalbumin antigen *ad lib* (Fig. 7A,S7A). One week following T cell transfer, we found reduced numbers of CD45.1$^+$ CD4$^+$ T cells in the mesenteric lymph node of OX40L$^{\Delta Rorc}$ mice compared to littermate controls, indicating a role for OX40L on intestinal ILC3s in regulating an antigen-specific T cell response.

At steady state, endogenous CD4$^+$ T cells from the intestinal lamina propria of OX40L$^{\Delta Rorc}$ mice showed equivalent RORγt$^+$ cells, but a significant reduction in T-bet$^+$ cells (Fig. 7B, S7B). To test if ILC3 expression OX40L regulated inflammatory T cell colitis, we used the T cell transfer colitis model. Induction of T cell-dependent disease has previously been shown to require OX40 on transferred T cells (Griseri et al., 2010). We sort-purified CD4$^+$CD45RB^{high} naïve T cells from WT mice into *Tnfsf4*$^{flox/flox}$ *Rorc-cre RAG2*$^{-/-}$ (called OX40L$^{\Delta ILC3}$) or *Tnfsf4*$^{fox/fox}$ *RAG2*$^{-/-}$ (called OX40L$^{\Delta ILC3}$) littermate controls. In contrast to littermate controls which showed a failure to gain weight and intestinal inflammatory infiltrates consistent with T cell colitis, OX40L-deficient mice continued to gain weight and showed no significant intestinal inflammation (Fig. 7C, D). Colonic CD4$^+$ T cell production of IFNγ and T-BET expression was significantly reduced in OX40L-deficient animals compared to controls (Fig. 7E, F). Given the role for TL1A signaling in regulating ILC3 expression of OX40L, we next tested the impact of DR3- deletion in the T cell transfer colitis model. Weight loss and reduced survival consistent with chronic T cell-mediated colitis developed within 4 weeks in the *RAG2*$^{-/-}$ littermate controls, but similar to the OX40L-deficient mice, ILC3-specific deletion of DR3 protected mice from T cell transfer colitis (Fig. 7G). No differences were observed in the microbiome composition of OX40L- or DR3-deficient mice compared to littermate controls (Fig. S7C, D). Analysis of colonic tissue in these mice revealed decreased histopathologic damage (Fig. 7H) and a significant reduction in T-BET$^+$ CD4$^+$ T cells (Fig. 7I) in the DR3$^{\Delta ILC3}$ mice compared to littermate controls. Thus, in contrast to the protective role for TL1A in acute colitis, these data reveal a pro-inflammatory role for ILC3-intrinsic DR3 in chronic T cell colitis.

DISCUSSION

Our data highlight the role for the IBD-linked gene *TNFSF15* and its protein TL1A as a central regulator of ILC3 function linking innate and adaptive immunity. Previous reports on the role for TL1A in inflammatory colitis offered contradicting results with TL1A promoting protection in acute models of colitis (Jia et al., 2016) and exacerbating T cell-dependent

inflammation in chronic colitis (Zheng et al., 2013). Using cell-specific genetic deletion models, our results now help to reconcile these findings, revealing a central role for ILC3 in mediating acute protection in acute colitis models (DSS and *Citrobacter rodentium* colitis), but promoting DR3-dependent pathogenic T cell responses in chronic disease (T cell transfer colitis). These findings highlight the protective role for TL1A in promoting mucosal healing during IBD (Bamias et al., 2003; Prehn et al., 2004). In synergy with IL-23, TL1A can act as a rheostat to regulate ILC3 effector functions. TL1A synergy with IL-23 in ILC3 required p38 MAPK, but no significant change in key transcription factors (R0Rγt, Ahr, Hif1a) or STAT3 phosphorylation was observed. The direct and indirect mechanistic targets of TL1A regulation of IL-22 in ILC3s still need to be defined. 0n a population level, genetic variants promoting this TL1A-dependent mucosal healing response may confer protection against infectious pathogens; however, sustained induction of TL1A, in patients with additional genetic susceptibility or environmental exposure, may support pathogenic T cell expansion (Zheng et al., 2013) or effector ILCs during chronic inflammation.

Our results support a key role for IBD-associated adherent bacteria in regulating MNPs as the main producers of intestinal TL1A. As sentinels of barrier immunity, MNPs integrate microbial signals and activate both innate and adaptive effector immunity. By producing IL-23 and IL-1β as well as CXCL16, MNPs are positioned functionally and spatially to rapidly coordinate ILC3 effector cytokine production (Longman et al., 2014; Satoh-Takayama et al., 2014). Adherent microbiota, including SFB and Adherent- invasive *E. coli,* induce TL1A consistent with their ability to potently induce ILC3 production of IL-22 (Sano et al., 2015; Viladomiu et al., 2017). These findings offer a mechanism by which Crohn's disease-associated microbiota can act acutely to promote barrier immunity in wild-type hosts. The adherence and metabolic characteristics of the intestinal microbiota may offer a novel approach for regulating TL1A effects in the mucosa.

The discovery of antigen processing and presentation by intestinal ILC3 highlights a central role for these cells in linking innate and adaptive immunity (Hepworth et al., 2013). Although splenic ILC3 can upregulate conventional co-stimulatory molecules CD80 and CD86 following IL-1β stimulation (von Burg et al., 2014), the absence of these co-stimulatory molecules following stimulation on intestinal ILC3s lead to a model in which they limit bacteria-specific inflammatory T cell responses in the gut (Hepworth et al., 2015). Our data demonstrate expression of OX40L by ILC3 after TL1A stimulation and highlight increased expression of 0X40L by ILC3 in inflammatory colitis in mouse models and human IBD. Expression of 0X40L by ILC3s plays a critical role in regulating gut antigen-specific and effector T cell responses. Although the total number of intestinal ILC3s are limited, functional and spatial organization of these cells facilitate efficient regulation of immunity in the tissue (Satoh- Takayama et al., 2014). These data, therefore, extend the model by which $MHCII^+$ ILC3s may regulate the intestinal T cell response. In IBD patients with genetic susceptibility or animal models of T cell transfer colitis, ILC3 co-stimulation can support pathogenic inflammatory T cell activation. Under homeostatic conditions, this model may extend to other 0X40L-dependent regulatory responses (Griseri et al., 2010). Recent studies have demonstrated significant heterogeneity in ILC3 populations, including $MHCII^+$ and $MHCII^-$ subsets (Bjorklund et al., 2016; Gury-BenAri et al., 2016; Lim et al., 2017). While our data show an essential role for ILC3-specific OX40L in mediating TLIA-dependent T

cell responses, further studies are needed to define intrinsic features of MHCII^{+} or MHCII^{-} ILC3 that contribute to their role in tissue specific T cell regulation.

These studies reveal a central role for TL1A in directing ILC3-dependent mucosal immunity. We now propose a model in which MNP-derived TL1A stimulation of intestinal ILC3 serves as a critical component linking innate and adaptive barrier immunity in colitis. During acute colitis, TL1A synergy with IL-23 promotes mucosal healing, but sustained intestinal damage leads to the upregulation of OX40L on ILC3 and co-stimulation of inflammatory intestinal T cells. Our data from IBD patients reveal a conserved TL1A - OX40L pathway in ILC3 with the potential to guide diagnostic and therapeutic approaches for IBD.

STAR METHODS

Experimental Models and Subject Details

Mice.—C57BL/6, *Itgax-cre, Rorc-cre, OT-II, illr*$^{-/-}$*, Cx3cr1-GFP, Cx3cr1-CreER* mice were purchased from The Jackson Laboratory. All mouse models were on C57BL/6 background. CX3CRI-DTR mice (Longman et al., 2014) were previously described. *Il23r*^{GFP} mice were obtained from M. Oukka (Awasthi et al., 2009). *Myd88*$^{-/-}$ were obtained from J. Blander. MHCII$^{\Delta ILC3}$ mice were obtained from G. Sonnenberg (Hepworth et al., 2015). *Tnfsf4*^{flox} were provided by T. Vyse and M. Botto (Cortini et al., 2017). *Tnfrsf25*$^{-/-}$ mice were obtained from Cancer Research UK (Wag et al., 2001). Generation of *Tnfrsf25*$^{flox/flox}$ mice is previously described (Shih et al., 2014). *Tnfsf15*$^{flox/flox}$ mice were generated at Cedars-Sinai by D. Shih and S. Targan. *Tnfsf15* endogenous locus containing 4.5 bp upstream and 3.4 bp downstream of exon 1 were generated by PCR amplification using proprietary C57BL/6J library developed at genOway. Subsequently, two loxP sites were inserted flanking exon 1. Positive selection neomycin gene flanked by FRT sites was inserted to the intron after exons 1 to generate the targeting vector. Every step of the cloning process was validated through restriction enzyme analysis and sequencing. The Tl1a gene targeting construct was linearized and electroporated into embryonic stem (ES) cells with C57BL/6J background. Homologous recombinants were selected by G418 and confirmed by PCR and Southern blot analysis. ES clones with correct 5' and 3' recombination were microinjected into C57BL/6J blastocysts and introduced into pseudopregnant C57BL/6J mice. Male chimeric offspring were bred to obtain germ line mutant mice, which were then bred to flpe delete mouse strain to remove the neomycin cassette and were confirmed by Southern blot. For CX_3CR1^{+} MNP depletion studies using Cx3cr1^{DTR} mice, diptheria toxin was i.p. injected (200ng/200uL) for two consecutive days and then every 72 hours to maintain depletion. For recombinant IL-22 rescue experiments of *DR3*$^{-/-}$ and *DR3*$^{\Delta ILC3}$, 5ug of rIL-22 was injected i.v. on days 4 and 6. All experiments were performed with 6–8 week old littermates. Both male and female mice were used with random and equal assignment of same sex to each experimental group. All vertebrate work was approved by the IACUC at Weill Cornell Medicine.

Human IBD subjects.

Endoscopic biopsies were obtained under an Institutional Review Board-approved protocol (1103011578) and informed consent was obtained at Weill Cornell Medicine (WCM)

including patients >18 years of age. Active inflammation was defined by an endoscopic score of >2 and inactive disease was defined by an endoscopic score of 0. The age and gender of subjects included are as follows: Healthy controls—22, 38, 53, 55, 71, 72, 79 year old males and 36 year old female; Crohn's inactive—30, 52, and 57 year old males; Crohn's active—32, 36 year old males and 27, 44, 55, 55, 62, and 68 year old females.

Method details

Antibodies and flow cytometry.

Staining of mouse cells was performed with CD3- FITC (145–2C11), CD4-eFluor780 (RM4–5), CD5-PE (53–7.3), CD45.1-APC (A20), CD90.2-efluor450 (53–2.1), MHCII-Alexa700 (M5/114.15.2), F4/80-PE (BM8), Ly6C- eFluor450 (HK1.4), CD19-FITC (MB19–1), CD11b-eFluor780 (M1/70), CD11c-PE-Cy7 (N418), CD103-APC (2E7), TCRγδ-FITC (11–5711-82), KLRG1-PE (2F1), NKp46- eFluor710 (29A1.4), OX40L-APC (RM134L), and ICOSL-eFluor660 (HK5.3), all from eBioscience. The following antibodies were purchased from BioLegend: CD127-PE- Cy7 (A7R34), CCR6-BV421 (29–2L17), DR3-PE (4C12). Intracellular mouse cytokine staining was performed with ROR0γt-PE (B2D), T-bet-e660 (eBio4B10), Foxp3-e450 (FJK-16s), IL-22-APC (IL22JOP), GMCSF-FITC (MP1–22E9), IL-13-PE-Cy7 (eBio13A), IL-17-PE (eBio17B7), IFNγ-PE-Cy7 (XMG1.2), TL1A-e710 (Tandys1a), all from eBioscience. Extracellular staining of human cells was performed with CD14-PE (61D3) and CD14-Alexa700 (63D3), HLA-DR-Alexa700 (LN3), TL1A-eFluor710 (Tandys1a), CD45-APC (2D1), CD3-eFluor780 (UCHT1), CD5-eFluor780 (UCHT2), CD19-Alexa700 (HIB19), CD11c-Alexa700 (3.9; Invitrogen), CD127-PE-Cy7 (eBioRDR5), ST2L-FITC (B4E6), CD117-efluor450 (104D2), OX40L-PE (11C3.1;Biolegend), all from eBioscience unless otherwise noted. Dead cells were excluded using the LiveIDead fixable aqua dead cell stain kit (Invitrogen). Cell proliferation was measured using CFSE (eBioscience). Phosphoflow was performed using pERK1I2-Pacific Blue (20A), pIKBa- e660 (RILYB3R), p38-MAPK-Alex647 (pT180IpY182). Intracellular cytokine staining was performed according to the manufacturer's protocol (CytofixICytoperm buffer set; BD) and transcription factor staining for was performed according to manufacturer's protocol (Intracellular Fixation and Permeabilization kit; eBioscience). Flow cytometry was performed with a BD LSRFortessa and analyzed with FlowJo software (Tree Star). Proliferation indexes were calculated as per FlowJo as the total number of divisions divided by the pool of dividing cells.

Preparation of LPMC.

Mouse intestines or human endoscopic biopsies were washed in PBS and 1 mM DTT with 30 mM EDTA, and then digested in collagenase 8 (Sigma- Aldrich) and DNase-containing media with 10% fetal bovine serum. Digested material was passed through a cell strainer and separated on a discontinuous 40%/80% Percoll gradient. LPMCs were cultured ex vivo in the presence of GolgiPlug (BD) for 4 h or stimulated with phorbol myristate acetate (PMA; 20 ng/ml) and ionomycin (1 μg/ml) or IL-23 (40 ng/ml; eBioscience) in the presence of GolgiPlug (BD) for 4 h before staining.

Intestinal ILC cultures.

Lineage$^-$ KLRG1$^-$ IL23R-GFP mouse ILC3 were sorted from LPMCs and resuspended in RPMI (10% FBS) tissue culture media for stimulation directly *ex vivo.* Mouse ILCs were stimulated with mouse recombinant IL-23 (eBioscience; 40 ng/ml), IL-1 (eBioscience; 10 ng/ml), or TL1A (R&D Systems; 200 ng/ml), as indicated. After 18 h, supernatants were harvested for IL-22 or GM-CSF ELISA (eBioscience) and Golgi Plug (BD) was added to cells for 4 h for subsequent intracellular cytokine staining.

Co-culture assays.

Sort-purified ILC3 (2×10^4) and MNP (1×10^4) populations were co-cultured in a 96-well round-bottom plate in tissue culture media. Cultures were incubated at 37^{o}C for 18h. Supernatants were harvested for ELISA and remaining cells were incubated with Golgi Plug (BD) for 4 hours and subsequently analyzed by flow cytometry. For antigen-specific T cell proliferation assays, 2×10^5 sort-purified, CFSE- labeled naive CD4$^+$ T cells from OTII transgenic mice were co-cultured with either 2.5×10^4 sort-purified ILC3 from IL23R$^{GFP/wt}$ mice or 2×10^4 MHCII$^+$CD11c$^+$CD11b$^+$ MNPs, with 20ug/mL OVA peptide (OVA 323–339; InvivoGen) and 200ng/mL rTL1A, as indicated, in a 96-well flat bottom plate. For co-stimulatory blocking assays, ILC3/Tcell co-cultures were blocked with 20ug/mL anti-mouse ICOSL antibody (LEAF purified anti-mouse CD275; BioLegend) or 15ug/mL anti-mouse 0X40L antibody (Biotin anti-mouse CD252; BioLegend).

Colitis models.

To induce chemical colitis in mice, 2% DSS (w/v) (M.W. 40,000–50,000; Affymetrix) was added to sterile drinking water and administered ad libitum for 7 days. After 7 days, DSS was replaced with normal drinking water. To induce infectious colitis, mice were orally gavaged with log phase growth *Citrobacter rodentium* DBS100 (ATCC 51459; American Type Culture Collection) at 1×10^{10} in PBS. For T cell transfer colitis, 5×10^5 CD4+ CD45RB^{high} CD25$^-$ CD62L$^-$ T cells were transferred into *DR3$^{\Delta ILC3}$* or *DR3$^{flox/flox}$* mice. For all colitis experiments, mice were monitored daily (DSS) or weekly (T cell transfer) for weight loss, rectal bleeding, diarrhea and survival throughout the experiments. For *in vivo* experiments using AIEC 2A, mice were pre-treated for 21 days with a broad-spectrum antibiotic cocktail of ampicillin (1 g/L), neomycin (0.5g/L), metronidazole (0.5g/L) and vancomycin (0.5g/L) in their drinking water. Mice were then orally gavaged with 2×10^9 of AIEC 2A before colitis induction with 2% DSS in their drinking water. For antigen-specific T cell transfer, 5×10^5 naive CD45.1$^+$ CD3$^+$CD4$^+$ CD44$^-$ CD25$^-$ CD62L$^+$Vα2$^+$ OTII T cells were sort purified and transferred i.p.

qPCR.

RNA from primary intestinal cell populations was prepared with TRIzol (Invitrogen) and purified RNA was reverse transcribed into cDNA (Quanta qScript). qPCR was performed with a QuantStudio 6 Flex Real-time PCR (Applied Biosystems) with SYBR Green Supermix (Bio-Rad Laboratories). The following primers were used: for *Reg3g,* 5'-GGGATCTGCAAGACAGACAAG-3' and 5'-GGGGCATCTTTCTTGGCAAC'3'; for *Saa1,* 5'-CATTTGTTCACGAGGCTTTCC-3' and 5'-

GTTTTTCCAGTTAGCTTCCTTCATGT-3'; for *Tnfsf15,* 5'-ATGCTTCGGGCCATAACAGA-3' and 5'-TGAAGGCCATCCCTAGGTCA-3'; for *Il22*, 5'- GCTCAGCTCCTGTCACATCA-3' and 5'-CAGTCCCCCAATCGCCTTGA-3'; for *0×40l,* 5'-GTGGTCTCTGGGATCAAGGG-3' and 5'-TCACATCTGGTAACTGCTCCTC-3'; for *Hprt,* 5'-GAGGAGTCCTGTTGATGTTGCCAG-3' 5'- GGCTGGCCTATAGGCTCATAGTGC-3' (Stephens et al., 2011). The thermocycler program was as follows: initial cycle of 95°C for 60s, followed 40 PCR cycles at 95°C for 5s, 60°C for 15s, 72°C for 15s. Relative levels of the target genes were determined by using the $\Delta\Delta C_t$ of the target gene compared to *Hprt* expression.

16S rRNA Gene Sequencing and Analyses.

16S rRNA gene sequencing methods were adapted from the methods developed for the Earth Microbiome Project (Caporaso et al., 2011). Briefly, bacterial genomic DNA was extracted using the Maxwell RSC (Promega). The 16S rDNA V4 and V5 regions were amplified by PCR and sequenced in the MiSeq platform (Illumina) using the 2×250 bp paired-end protocol (Caporaso et al., 2012). The read pairs were demultiplexed based on the unique molecular barcodes, and reads were merged using USEARCH 10.0.240 (Edgar, 2010). Taxonomic labelling of OUT representative sequences was carried out with a confidence threshold of 0.8, using the Ribosomal Database Project training set (version 16) (Cole et al., 2014). A rarefied OTU table from the output files generated in the previous two steps was used for downstream analyses of α-diversity, β-diversity (Lozupone and Knight, 2005), and phylogenetic trends.

Quantification and Statistical Analysis

RNA-seq analysis.—Mouse RNA-Seq data was aligned to the mm10 assembly of the mouse genome using the STAR aligner[1]. Read counts for genes across all BAM files were computed using the HTSeq software[2]. Differential analysis of RNA-Seq samples utilized the DESeq package for gene expression analysis[3]. False discovery rate correction of P-values used for all bioinformatics analyses of this study utilized the Benjamini-Hochberg procedure[4]. Heatmap clustering and production was done using the heatmap function within the NMF package in **R**[5]. Principal components analysis plots were visualized using the ggbiplot package in **R**.

Statistical analysis.

Statistical analysis was performed in GraphPad Prism or R software. Results represent mean ± s.e.m. and were analyzed by unpaired Student's t- test, Mann-Whitney test, one-way ANOVA, Log-rank (Mantel-Cox) test, as indicated in the figure legends. Given that mouse experiments required littermate controls and complex genotyping, experimental group allocation was not blinded. No relevant exclusion criteria were applied.

Supplementary Material

Refer to Web version on PubMed Central for supplementary material.

Acknowledgments:

We would like to acknowledge Timothy Vyse and Marina Botto (*Tnfsf4*$^{flox/flox}$), Julie Blander (*MyD88*$^{-/-}$), and Gregory Sonnenberg *(H2-Ab1*$^{flox/flox}$ *Rorc-cre)* for generously providing mice. Bioinformatics support was provided by the Jill Roberts Institute for Research in IBD and microbiome sequencing was performed by the Microbiome Core Lab at Weill Cornell Medicine. We would like to thank Gregory Sonnenberg for helpful comments and critical review of the manuscript.

Funding: This work was supported by grants from the Crohn's and Colitis Foundation Senior Research Award (R.S.L), NIH 1R03DK111852 and 1R01 DK114252 (R.S.L), NIHR01AI125264 (G.E.D.), USPHS grant DK056328 (S.R.T.), NIH K08 Career Development Award DK099381 (R.S.L) and DK093578 (D.Q.S.), NIH Medical Scientist Training Program grant T32GM07739 (J.G.C.) and the F. Widjaja Foundation Inflammatory Bowel & Immunobiology Research Institute (S. R. T. and D. Q. S).

References:

Ahn YO, Weeres MA, Neulen ML, Choi J, Kang SH, Heo DS, Bergerson R, Blazar BR, Miller JS, and Verneris MR (2015). Human group3 innate lymphoid cells express DR3 and respond to TL1A with enhanced IL-22 production and IL-2-dependent proliferation. Eur J Immunol 45, 2335–2342. [PubMed: 26046454]

Awasthi A, Riol-Blanco L, Jager A, Korn T, Pot C, Galileos G, Bettelli E, Kuchroo VK, and Oukka M (2009). Cutting edge: IL-23 receptor gfp reporter mice reveal distinct populations of IL-17-producing cells. J Immunol 182, 5904–5908. [PubMed: 19414740]

Bamias G, Jia LG, and Cominelli F (2013). The tumor necrosis factor-like cytokine 1A/death receptor 3 cytokine system in intestinal inflammation. Curr Opin Gastroenterol 29, 597–602. [PubMed: 24100723]

Bamias G, Martin C, 3rd, Marini M, Hoang S, Mishina M, Ross WG, Sachedina MA, Friel CM, Mize J, Bickston SJ, et al. (2003). Expression, localization, and functional activity of TL1A, a novel Th1-polarizing cytokine in inflammatory bowel disease. J Immunol 171, 4868–4874. [PubMed: 14568967]

Basu R, O'Quinn DB, Silberger DJ, Schoeb TR, Fouser L, Ouyang W, Hatton RD, and Weaver CT (2012). Th22 cells are an important source of IL-22 for host protection against enteropathogenic bacteria. Immunity 37, 1061–1075. [PubMed: 23200827]

Bjorklund AK, Forkel M, Picelli S, Konya V, Theorell J, Friberg D, Sandberg R, and Mjosberg J (2016). The heterogeneity of human CD127(+) innate lymphoid cells revealed by single-cell RNA sequencing. Nat Immunol 17, 451–460. [PubMed: 26878113]

Caporaso JG, Lauber CL, Walters WA, Berg-Lyons D, Huntley J, Fierer N, Owens SM, Betley J, Fraser L, Bauer M, et al. (2012). Ultra-high-throughput microbial community analysis on the Illumina HiSeq and MiSeq platforms. Isme J 6, 1621–1624. [PubMed: 22402401]

Caporaso JG, Lauber CL, Walters WA, Berg-Lyons D, Lozupone CA, Turnbaugh PJ, Fierer N, and Knight R (2011). Global patterns of 16S rRNA diversity at a depth of millions of sequences per sample. Proc Natl Acad Sci U S A 108 Suppl 1, 4516–4522. [PubMed: 20534432]

Cole JR, Wang Q, Fish JA, Chai B, McGarrell DM, Sun Y, Brown CT, Porras-Alfaro A, Kuske CR, and Tiedje JM (2014). Ribosomal Database Project: data and tools for high throughput rRNA analysis. Nucleic Acids Res 42, D633–642. [PubMed: 24288368]

Cortini A, Ellinghaus U, Malik TH, Cunninghame Graham DS, Botto M, and Vyse TJ (2017). B cell 0X40L supports T follicular helper cell development and contributes to SLE pathogenesis. Ann Rheum Dis 76, 2095–2103. [PubMed: 28818832]

Diehl GE, Longman RS, Zhang JX, Breart B, Galan C, Cuesta A, Schwab SR, and Littman DR (2013). Microbiota restricts trafficking of bacteria to mesenteric lymph nodes by CX(3)CR1(hi) cells. Nature 494, 116–120. [PubMed: 23334413]

Edgar RC (2010). Search and clustering orders of magnitude faster than BLAST. Bioinformatics 26, 2460–2461. [PubMed: 20709691]

Gevers D, Kugathasan S, Denson LA, Vazquez-Baeza Y, Van Treuren W, Ren B, Schwager E, Knights D, Song SJ, Yassour M, et al. (2014). The treatment-naive microbiome in new-onset Crohn's disease. Cell Host Microbe 15, 382–392. [PubMed: 24629344]

Griseri T, Asquith M, Thompson C, and Powrie F (2010). 0X40 is required for regulatory T cell-mediated control of colitis. J Exp Med 207, 699–709. [PubMed: 20368580]

Gury-BenAri M, Thaiss CA, Serafini N, Winter DR, Giladi A, Lara-Astiaso D, Levy M, Salame TM, Weiner A, David E, et al. (2016). The Spectrum and Regulatory Landscape of Intestinal Innate Lymphoid Cells Are Shaped by the Microbiome. Cell 166, 1231–1246 e1213. [PubMed: 27545347]

Hedl M, and Abraham C (2014). A TNFSF15 disease-risk polymorphism increases pattern-recognition receptor- induced signaling through caspase-8-induced IL-1. Proc Natl Acad Sci U S A 111, 13451–13456. [PubMed: 25197060]

Hepworth MR, Fung TC, Masur SH, Kelsen JR, McConnell FM, Dubrot J, Withers DR, Hugues S, Farrar MA, Reith W, et al. (2015). Immune tolerance. Group 3 innate lymphoid cells mediate intestinal selection of commensal bacteria-specific CD4(+) T cells. Science 348, 1031–1035. [PubMed: 25908663]

Hepworth MR, Monticelli LA, Fung TC, Ziegler CG, Grunberg S, Sinha R, Mantegazza AR, Ma HL, Crawford A, Angelosanto JM, et al. (2013). Innate lymphoid cells regulate CD4 T-cell responses to intestinal commensal bacteria. Nature.

Ivanov II, Atarashi K, Manel N, Brodie EL, Shima T, Karaoz U, Wei D, Goldfarb KC, Santee CA, Lynch SV, et al. (2009). Induction of intestinal Th17 cells by segmented filamentous bacteria. Cell 139, 485–498. [PubMed: 19836068]

Jia LG, Bamias G, Arseneau KO, Burkly LC, Wang EC, Gruszka D, Pizarro TT, and Cominelli F (2016). A Novel Role for TL1A/DR3 in Protection against Intestinal Injury and Infection. J Immunol 197, 377–386. [PubMed: 27233964]

Kaplan GG (2015). The global burden of IBD: from 2015 to 2025. Nat Rev Gastroenterol Hepatol 12, 720–727. [PubMed: 26323879]

Kim M, Galan C, Hill AA, Wu WJ, Fehlner-Peach H, Song HW, Schady D, Bettini ML, Simpson KW, Longman RS, et al. (2018). Critical Role for the Microbiota in CX3CR1(+) Intestinal Mononuclear Phagocyte Regulation of Intestinal T Cell Responses. Immunity.

Kinnebrew MA, Buffie CG, Diehl GE, Zenewicz LA, Leiner I, Hohl TM, Flavell RA, Littman DR, and Pamer EG (2012). Interleukin 23 production by intestinal CD103(+)CD11b(+) dendritic cells in response to bacterial flagellin enhances mucosal innate immune defense. Immunity 36, 276–287. [PubMed: 22306017]

Lim AI, Li Y, Lopez-Lastra S, Stadhouders R, Paul F, Casrouge A, Serafini N, Puel A, Bustamante J, Surace L, et al. (2017). Systemic Human ILC Precursors Provide a Substrate for Tissue ILC Differentiation. Cell 168, 1086–1100 e1010. [PubMed: 28283063]

Longman RS, Diehl GE, Victorio DA, Huh JR, Galan C, Miraldi ER, Swaminath A, Bonneau R, Scherl EJ, and Littman DR (2014). CX3CR1+ mononuclear phagocytes support colitis-associated innate lymphoid cell production of IL-22. J Exp Med 211, 1571–1583. [PubMed: 25024136]

Lozupone C, and Knight R (2005). UniFrac: a new phylogenetic method for comparing microbial communities. Appl Environ Microbiol 71, 8228–8235. [PubMed: 16332807]

McGovern DP, Kugathasan S, and Cho JH (2015). Genetics of Inflammatory Bowel Diseases. Gastroenterology 149, 1163–1176 e1162. [PubMed: 26255561]

Melo-Gonzalez F, and Hepworth MR (2017). Functional and phenotypic heterogeneity of group 3 innate lymphoid cells. Immunology 150, 265–275. [PubMed: 27935637]

Meylan F, Hawley ET, Barron L, Barlow JL, Penumetcha P, Pelletier M, Sciume G, Richard AC, Hayes ET, Gomez-Rodriguez J, et al. (2014). The TNF-family cytokine TL1A promotes allergic immunopathology through group 2 innate lymphoid cells. Mucosal Immunol 7, 958–968. [PubMed: 24368564]

Niess JH, Brand S, Gu X, Landsman L, Jung S, McCormick BA, Vyas JM, Boes M, Ploegh HL, Fox JG, et al. (2005). CX3CR1-mediated dendritic cell access to the intestinal lumen and bacterial clearance. Science 307, 254–258. [PubMed: 15653504]

Panea C, Farkas AM, Goto Y, Abdollahi-Roodsaz S, Lee C, Koscso B, Gowda K, Hohl TM, Bogunovic M, and Ivanov II (2015). Intestinal Monocyte-Derived Macrophages Control Commensal-Specific Th17 Responses. Cell Rep 12, 1314–1324. [PubMed: 26279572]

Prehn JL, Mehdizadeh S, Landers CJ, Luo X, Cha SC, Wei P, and Targan SR (2004). Potential role for TL1A, the new TNF-family member and potent costimulator of IFN-gamma, in mucosal inflammation. Clin Immunol 112, 66–77. [PubMed: 15207783]

Richard AC, Ferdinand JR, Meylan F, Hayes ET, Gabay O, and Siegel RM (2015). The TNF-family cytokine TL1A: from lymphocyte costimulator to disease co-conspirator. J Leukoc Biol 98, 333–345. [PubMed: 26188076]

Sano T, Huang W, Hall JA, Yang Y, Chen A, Gavzy SJ, Lee JY, Ziel JW, Miraldi ER, Domingos AI, et al. (2015). An IL-23R/IL-22 Circuit Regulates Epithelial Serum Amyloid A to Promote Local Effector Th17 Responses. Cell 163, 381–393. [PubMed: 26411290]

Satoh-Takayama N, Serafini N, Verrier T, Rekiki A, Renauld JC, Frankel G, and Di Santo JP (2014). The Chemokine Receptor CXCR6 Controls the Functional Topography of Interleukin-22 Producing Intestinal Innate Lymphoid Cells. Immunity 41, 776–788. [PubMed: 25456160]

Shih DQ, Kwan LY, Chavez V, Cohavy O, Gonsky R, Chang EY, Chang C, Elson CO, and Targan SR (2009). Microbial induction of inflammatory bowel disease associated gene TL1A (TNFSF15) in antigen presenting cells. Eur J Immunol 39, 3239–3250. [PubMed: 19839006]

Shih DQ, Zheng L, Zhang X, Zhang H, Kanazawa Y, Ichikawa R, Wallace KL, Chen J, Pothoulakis C, Koon HW, and Targan SR (2014). Inhibition of a novel fibrogenic factor Tl1a reverses established colonic fibrosis. Mucosal Immunol 7, 1492–1503. [PubMed: 24850426]

Siakavellas SI, and Bamias G (2015). Tumor Necrosis Factor-like Cytokine TL1A and Its Receptors DR3 and DcR3: Important New Factors in Mucosal Homeostasis and Inflammation. Inflamm Bowel Dis 21, 2441–2452. [PubMed: 26099067]

Sonnenberg GF, Monticelli LA, Elloso MM, Fouser LA, and Artis D (2011). CD4(+) lymphoid tissue-inducer cells promote innate immunity in the gut. Immunity 34, 122–134. [PubMed: 21194981]

Stephens AS, Stephens SR, and Morrison NA (2011). Internal control genes for quantitative RT-PCR expression analysis in mouse osteoblasts, osteoclasts and macrophages. BMC Res Notes 4, 410. [PubMed: 21996334]

Tung CC, Wong JM, Lee WC, Liu HH, Chang CH, Chang MC, Chang YT, Shieh MJ, Wang CY, and Wei SC (2014). Combining TNFSF15 and ASCA IgA can be used as a predictor for the stenosis/perforating phenotype of Crohn's disease. J Gastroenterol Hepatol 29, 723–729. [PubMed: 24783249]

Viladomiu M, Kivolowitz C, Abdulhamid A, Dogan B, Victorio D, Castellanos JG, Woo V, Teng F, Tran NL, Sczesnak A, et al. (2017). IgA-coated E. coli enriched in Crohn's disease spondyloarthritis promote TH17-dependent inflammation. Sci Transl Med 9.

von Burg N, Chappaz S, Baerenwaldt A, Horvath E, Bose Dasgupta S, Ashok D, Pieters J, Tacchini-Cottier F, Rolink A, Acha-Orbea H, and Finke D (2014). Activated group 3 innate lymphoid cells promote T- cell-mediated immune responses. Proc Natl Acad Sci U S A 111, 12835–12840. [PubMed: 25136120]

Wang EC, Thern A, Denzel A, Kitson J, Farrow SN, and Owen MJ (2001). DR3 regulates negative selection during thymocyte development. Mol Cell Biol 21, 3451–3461. [PubMed: 11313471]

Yang DH, Yang SK, Song K, Hong M, Park SH, Lee HS, Kim JB, Lee HJ, Park SK, Jung KW, et al. (2014). TNFSF15 is an independent predictor for the development of Crohn's disease-related complications in Koreans. J Crohns Colitis 8, 1315–1326. [PubMed: 24835165]

Zheng L, Zhang X, Chen J, Ichikawa R, Wallace K, Pothoulakis C, Koon HW, Targan SR, and Shih DQ (2013). Sustained Tl1a Expression on Both Lymphoid and Myeloid Cells Leads to Mild Spontaneous Intestinal Inflammation and Fibrosis. Eur J Microbiol Immunol (Bp) 3, 11–20. [PubMed: 23638306]

Zigmond E, Varol C, Farache J, Elmaliah E, Satpathy AT, Friedlander G, Mack M, Shpigel N, Boneca IG, Murphy KM, et al. (2012). Ly6C hi monocytes in the inflamed colon give rise to proinflammatory effector cells and migratory antigen-presenting cells. Immunity 37, 1076–1090. [PubMed: 23219392]

Highlights

- IBD-associated adherent microbiota induce MNP-derived TL1A
- MNP-derived TL1A promotes the ILC3-IL-22 axis and protects against acute colitis
- TL1A induces ILC3 expression of OX40L during colitis *in vivo*
- OX40L on ILC3s stimulates T cell activation and is required for T cell-driven colitis

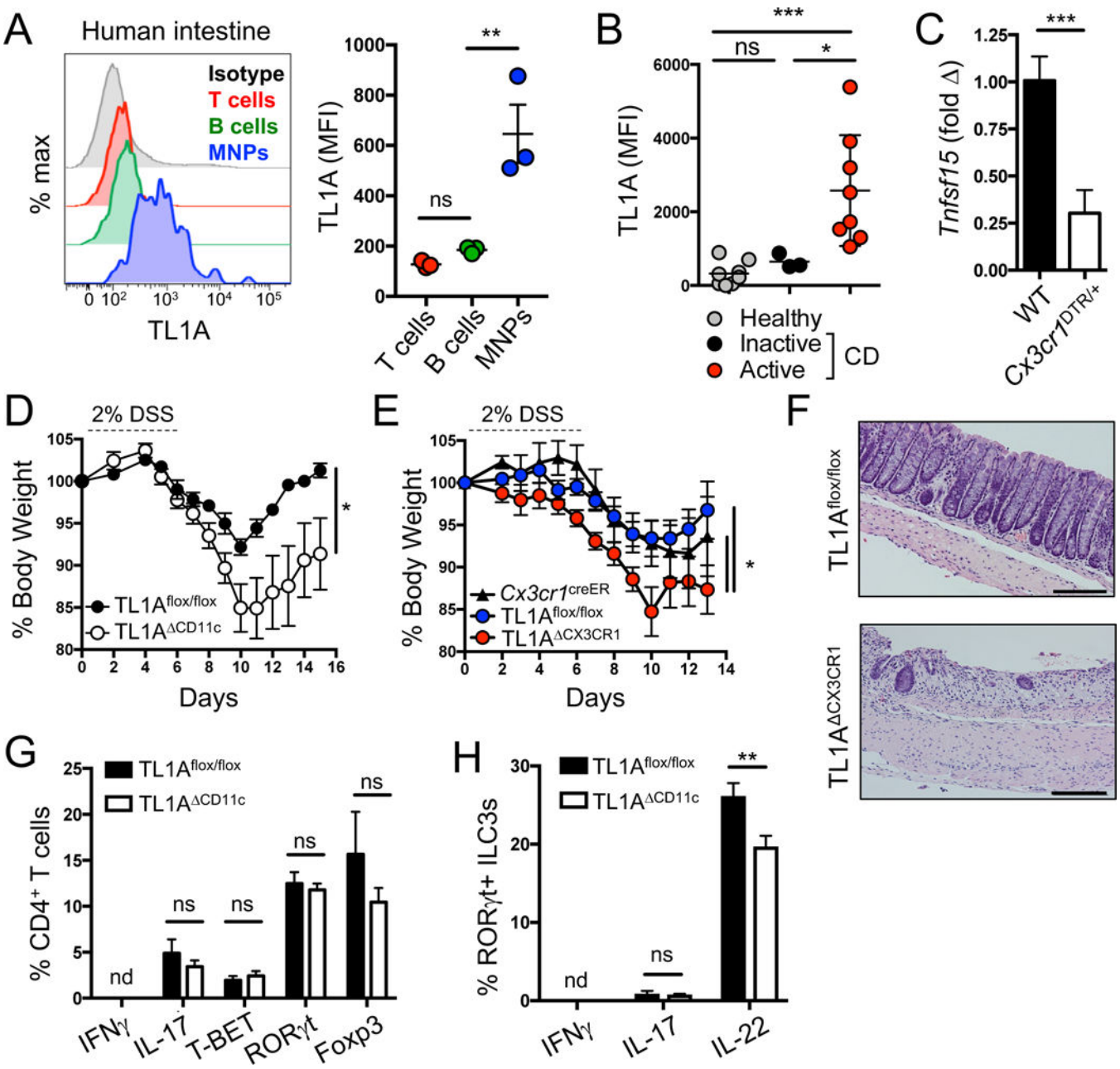

Fig. 1. MNP-derived TL1A promotes ILC3 IL-22 and protects against acute colitis.

(A) TL1A surface expression on CD3$^+$ T cells, CD19$^+$ B cells, and CD14$^+$ HLA-DR$^+$ MNPs from human intestinal biopsy (N=3). (**B**) MFI of TL1A surface expression on CD14$^+$ HLA-DR$^+$ MNPs (Healthy=8, Crohn's inactive=3, Crohn's active=8) measured by flow cytometry. (**C**) *Tnfsf15* expression by qPCR from intestinal cells from *Cx3cr1*$^{DTR/+}$ mice or WT controls after DT toxin injection (N=5 mice/group). (**D**) Weight loss curves of 2% DSS-treated *Tnfsf15*$^{flox/flox}$*Itgax-cre* (called TL1A$^{\Delta CD11c}$, N=9) *or Tnfsf15*$^{flox/flox}$ (called TL1A$^{flox/flox}$ N=10) littermate mice. Data are pooled from two independent experiments. (**E**) Weight loss curves of 2% DSS-treated TL1A^{floxIflox} (N=15), *Tnfsf15*$^{flox/flox}$ *Cx3cr1-creER* (called TL1A$^{\Delta CX3CR1}$J (N=12), or *Cx3cr1*^{CreER} (N= 5) littermate mice. Data are

pooled from three independent experiments. (**F**) Representative colonic histology from $TL1A^{\Delta CX3CR1}$ or $TL1A^{floxIflox}$ mice littermate mice following 2% DSS treatment for 9 days (scale bar: 100μm). (**G, H**) Flow cytometric analysis of intracellular cytokine staining (IFNγ, IL-17) or transcription factor (T-BET, RORγt) in $CD4^+$ T cells (G) or intracellular cytokine staining (IFNγ, IL-17, or IL-22) in $ROR\gamma t^+$ ILC3 from $TL1A^{floxIflox}$ or $TL1A^{\Delta CD11c}$ mice on day 3 after starting 2% DSS treatment (N=5 miceIgroup). Data are mean ± SEM and analyzed by ANOVA (A, B), two-tailed Student's t-test (C, G, and H), two-tailed Mann-Whitney test (D), or ANOVA with multiple comparisons test (E); $*P<0.05$, $**P<0.01$, $***P<0.001$. See also Figure S1.

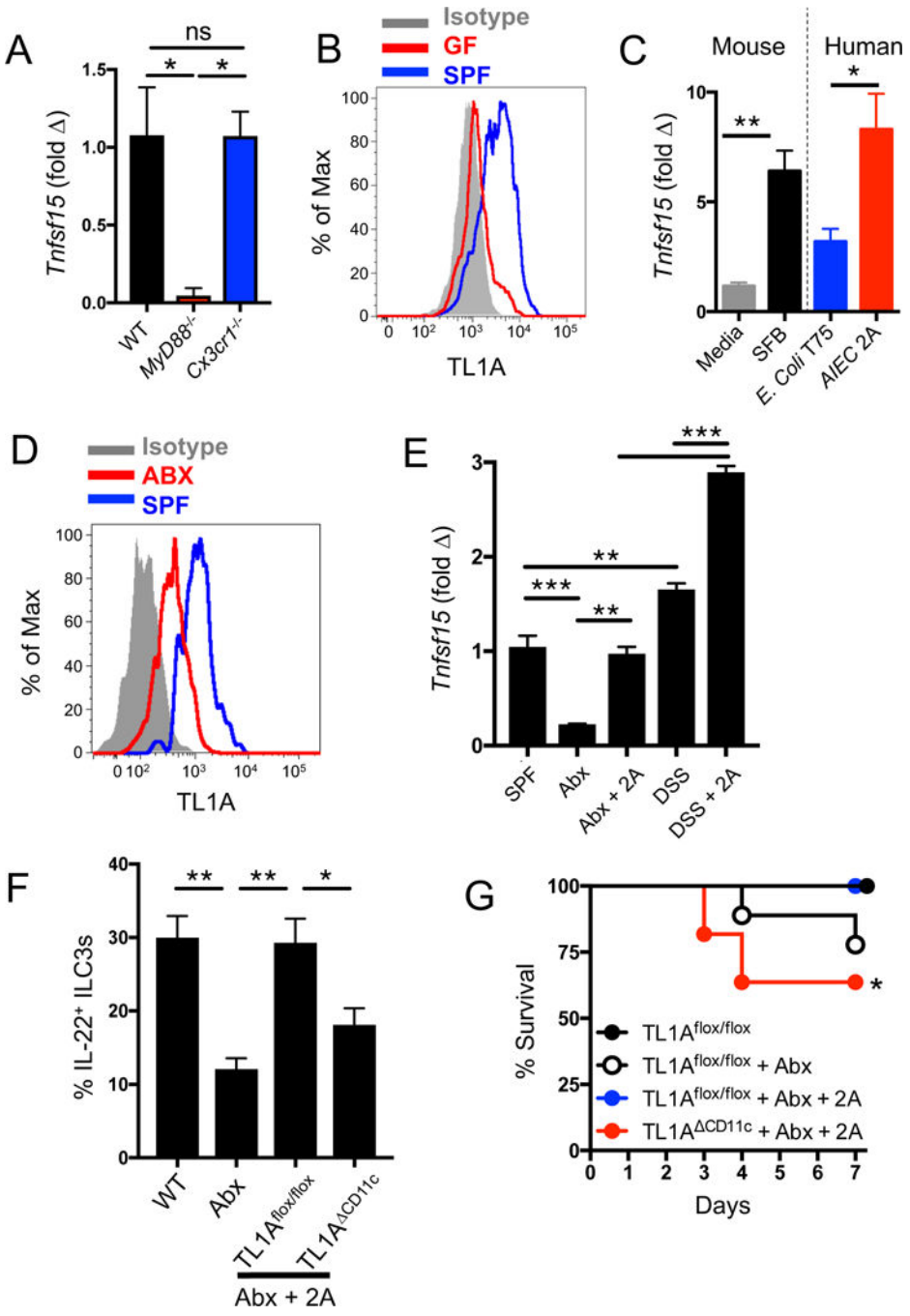

Fig. 2. IBD-associated adherent microbiota induce MNP-derived TL1A and promote protection in acute colitis.

(A) *Tnfsf15* expression by qPCR in MHCII^{+}CD11c^{+}CD11b^{+} MNPs sorted from WT, MyD88-deficient, or CX3CR1-deficient mice (N=3 mice/group). (**B**) Flow cytometric analysis of TL1A expression in MHCII^{+}CD11c^{+}CD11b^{+} MNP from germ-free (GF) or specific-pathogen-free (SPF) mice. (**C**) WT mice were mono-colonized with media control, SFB, non-adherent *E. coli* T75, *Adherent-invasive E. coli* 2A for 5 days. MNPs were sorted from the lamina propria and *Tnfsf15* expression determined by quantitative PCR (N=3–5

mice/group). One representative of two experiments is shown. (**D**) Flow cytometric analysis of TL1A expression in MHCII^{+}CD11c^{+}CD11b^{+}CX3CR1^{+} MNP from antibiotic-treated (ABX) or untreated specific-pathogen-free (SPF) *Cx3cr1*$^{GFP/WT}$ mice. One of three representative experiments is shown. (**E**) *Tnfsf15* expression by qPCR in MHCII^{+}CD11c^{+}CD11b^{+} MNPs sorted from WT SPF mice pre-treated with or without broad-spectrum antibiotics (Abx) for 3 weeks prior to subsequent AIEC 2A colonization (2A) or DSS for 5 days (N=3–5 miceIgroup). Data are pooled from two experiments. (**F**) IL-22 production by ILC3 from WT (N=6), *Tnfsf15*$^{flox/flox}$ (called TL1A^{floxIflox}, N=6), *or Tnfsf15*$^{flox/flox}$ *Itgax-cre* (TL1A$^{\Delta CD11c}$, N=8) mice pre-treated with or without broad-spectrum antibiotics (Abx) for 3 weeks prior to subsequent AIEC 2A colonization (2A). Data are pooled from two experiments. (**G**) TL1A^{floxIflox} and TL1A$^{\Delta CD11c}$ were pre-treated with broad-spectrum antibiotics for three weeks before colonization with 2A *E. coli.* Mice were then treated with 2% DSS for 7 days. Percent survival is shown. Data are pooled from two experiments. Data in A, C, E, and F are mean ± SEM and were analyzed by ANOVA (A, E, and F), two-tailed Student's t-test (C), or Log-rank (Mantel-Cox) test (G); $*P<0.05$, $**P<0.01$, $***P<0.001$.

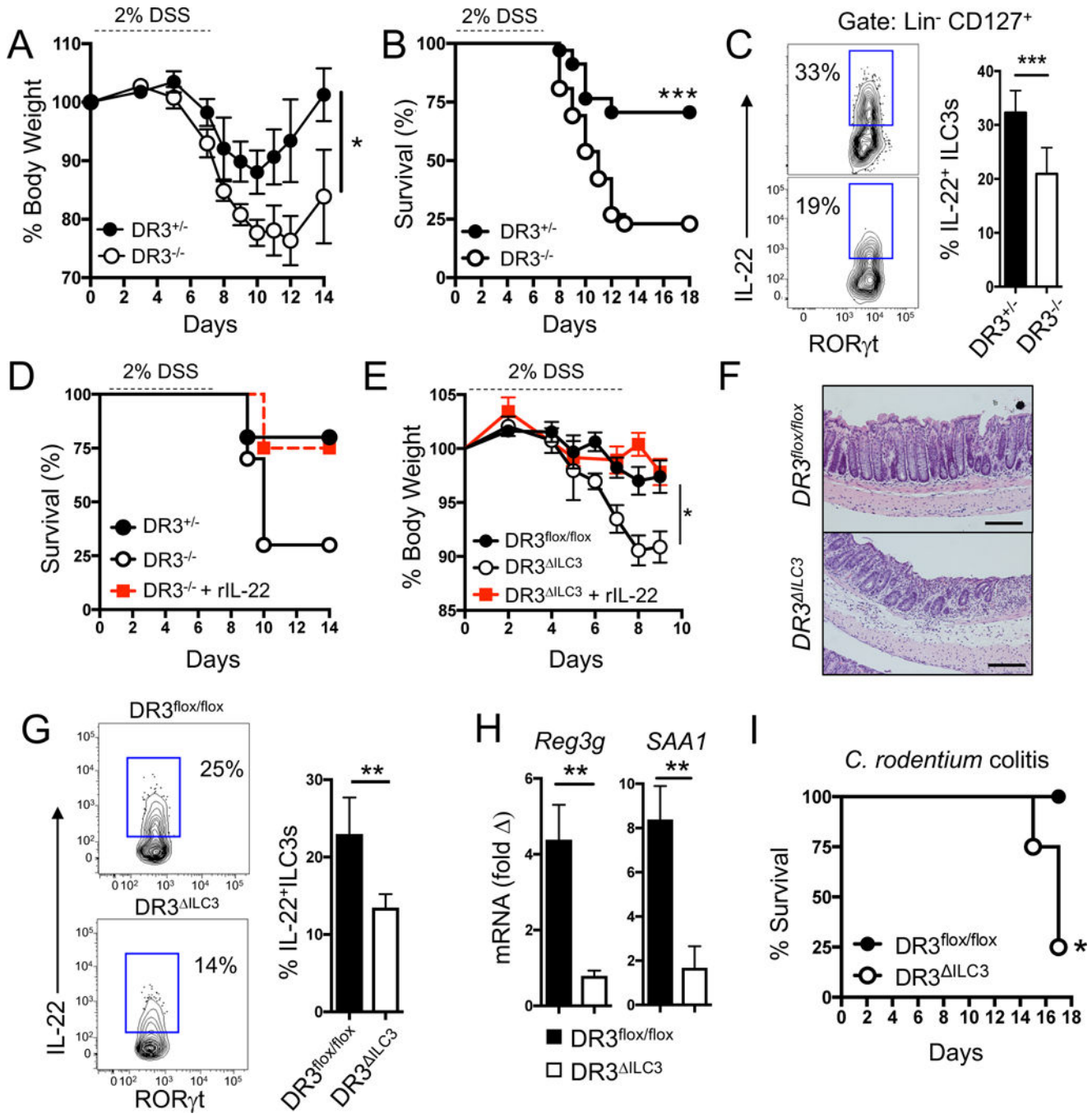

Fig. 3. ILC3 expression of DR3 plays an essential role in regulating IL-22- dependent protection from experimental colitis.

(**A, B**) Body weights (A) and percent survival curves (B) of *Tnfrsf25*$^{+/-}$ (called DR3$^{+/-}$, N=34) and *Tnfrsf25*$^{-/-}$ (called DR3$^{-/-}$, N=25) littermate mice following 7 day treatment with 2% DSS. Data are compiled from three independent experiments. (**C**) Percentage of colonic Lin^{-} CD127^{+}CD90^{+}R0Rγt^{+} ILC3s producing IL-22 from DSS-treated DR3$^{+/-}$ and DR3$^{-/-}$ co-housed littermate mice 9 days after starting DSS treatment (N=4–5 mice/group). (**D**) Percent survival of DR3$^{+/-}$ (N=5) and DR3$^{-/-}$ (N=4) littermate mice following 7 day

treatment with 2% DSS. i.v. rIL-22 was given on days 4 and 6 following initiation of DSS (N=4). (**E**) Body weights of 2% DSS-treated *Tnfrsf25*$^{flox/flox}$ *RAG2*$^{-/-}$ (called DR3$^{flox/flox}$, N=13) and *Tnfrsf25*$^{flox/flox}$ *Rorc-cre RAG2*$^{-/-}$ (called DR3$^{\Delta ILC3}$, N=13) littermate mice compared with DR3$^{\Delta ILC3}$ mice treated with rIL-22 i.v. on days 4 and 6 of DSS treatment (N=4). Data are compiled from two independent experiments. (**F**) Representative colonic histology from DR3$^{flox/flox}$ and DR3$^{\Delta ILC3}$ littermate mice following 2% DSS treatment for 7 days (analyzed in E). (**G**) Representative flow cytometry and pooled analysis of IL-22 production by ILC3s from DR3$^{flox/flox}$ (N=10) and DR3$^{\Delta ILC3}$ (N=5) littermate mice on day 3 after starting 2% DSS treatment. Data are compiled from two independent experiments. (**H**) Epithelial cell *Reg3g* and *SAA1* mRNA expression in 2% DSS-treated *dr3*$^{flox/flox}$ and *DR3*$^{\Delta ILC3}$ littermate mice 9 days after starting 2% DSS treatment (N=4 mice/group). Data are compiled from two independent experiments. (**I**) Percent survival of *C. rodentium-infected* DR3$^{flox/flox}$ and DR3 ^{3} littermate mice (N=5, 4 mice/group, respectively). Data in A, C, E, G, and H are mean ± SEM and analyzed by Mann-Whitney test (A, E); Log-rank (Mantel-Cox) test (B,D,I), or two-tailed Student's t-test (C, G, H); **P*<0.05, ***P*<0.01, ****P*<0.001. See also Figure S2 and S3.

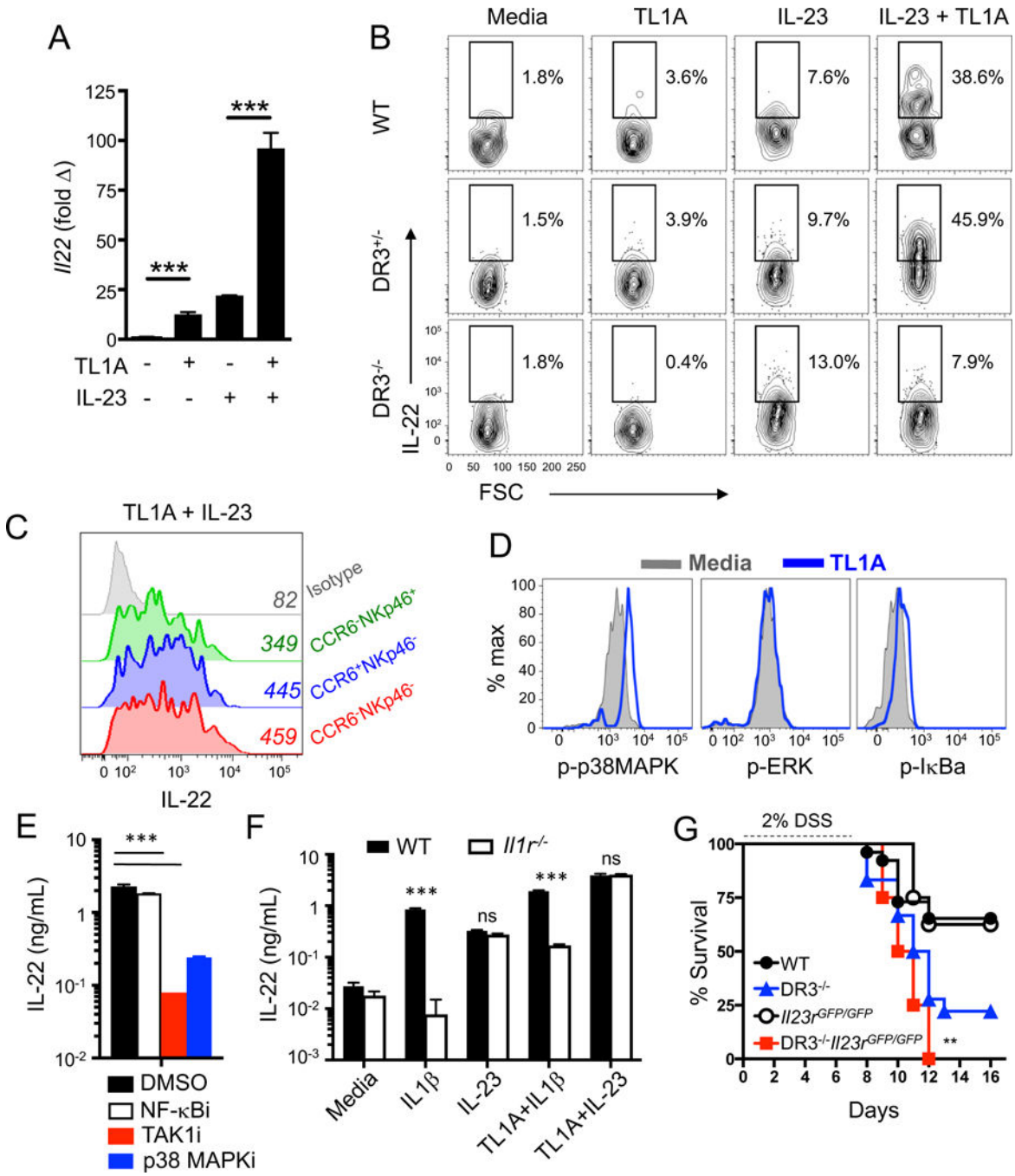

Fig. 4. TL1A potently and selectively synergizes with IL-23 via MAPK to induce IL- 22 production in ILC3 *in vitro* and *in vivo*.

(**A, B**) Sorted ILC3s from the intestinal lamina propria from WT, *Tnfrsf25*$^{+I-}$ (called DR3$^{+/-}$) or *Tnfrsf25*$^{-/-}$(called DR3$^{-/-}$) mice were stimulated *ex vivo* with media (−), rIL-23 and/or rTL1A. Quantitative PCR (A) or intracellular cytokine staining for IL-22 (B) was performed after 18h stimulation. One of three independent experiments is shown. (**C**) IL-22 production by sorted ILC3 subsets was measured by intracellular flow cytometry after 18h stimulation. Brefeldin was added to the cultures 4h before intracellular cytokine staining.

One of two independent experiments is shown. (**D**) Intracellular phosphoflow analysis was performed on sorted ILC3 for phosphorylation of p38-MAPK, ERK and IκBa 30 minute following stimulation. One of two independent experiments is shown. (**E**) Sorted ILC3s were stimulated for with rIL-23 and rTL1A in the presence of the indicated soluble inhibitors or control carrier DMSO (NF-κB inhibitor, NBD, white; TAK1 inhibitor, 5Z-7-Oxozeaenol, red; p38 MAPK inhibitor, SB203580, blue). IL-22 production was evaluated by ELISA. One of three independent experiments is shown. (**F**) IL-22 production by sorted ILC3s from WT or *Il1r*$^{-/-}$mice after 18 hour stimulation with media, rIL-1β, rTL1A, or rIL-23 (or in combinations). (**G**) Survival curves of WT, DR3$^{-/-}$, *Il23r*$^{GFP/GFP}$and *Tnfrsf25*$^{-/-}$ *Il23r*$^{GFP/GFP}$ (called DR3$^{-/-}$ *I/23r*$^{GFP/GFP}$*)* mice following 7 day treatment with 2% DSS. Data in are compiled from two independent experiments (with N=26, 18, 7, and 4 mice/group, respectively). Data in A, E, and F are mean ± SEM and analyzed by ANOVA (A, E) or two-tailed Student's t-test with Bonferroni correction. Data in G are analyzed by Log-rank (Mantel-Cox) test; ***P*<0.01, ****P*<0.001. See also Figure S4.

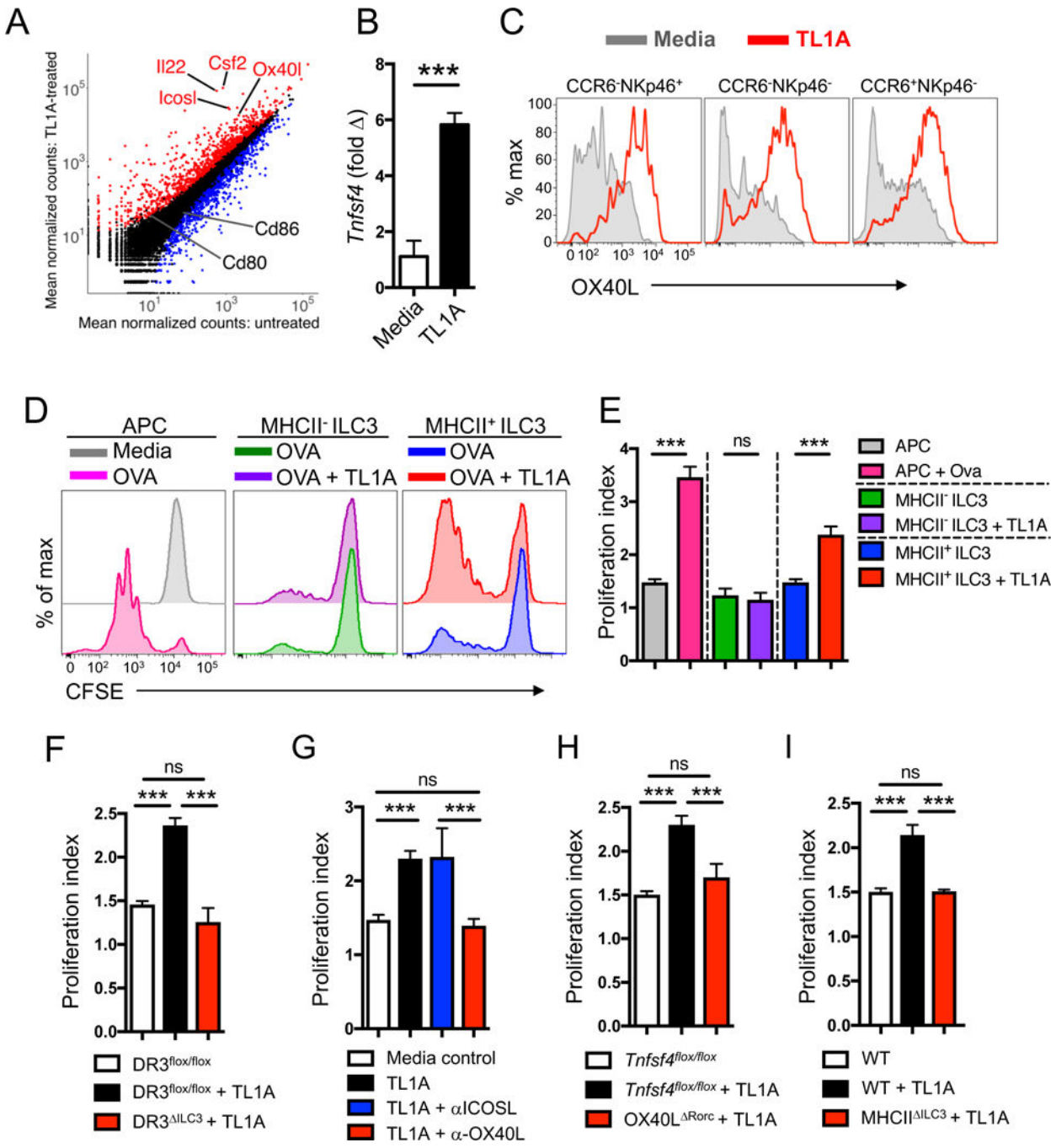

Fig. 5. TL1A induces OX40L-dependent stimulation of CD4$^+$ T cells by MHCII$^+$ ILC3s.

(**A**) Scatterplot of global gene expression profiles of media- or rTLIA-stimulated sorted Lin$^-$ CD127$^+$IL23R$^+$ILC3s from *Il23r*$^{GFP/WT}$ mice. Red and blue dots indicate significantly up- or down-regulated genes, respectively, after FDR correction for multiple hypothesis testing. Data are compiled from two independent experiments. (**B, C**) *Tnfsf4* mRNA expression (B) and 0X40L surface protein (C) in sorted Lin$^-$CD127$^+$IL23R^{GFP+} ILC3s from *Il23r*$^{GFP/WT}$ mice stimulated for 18 hours with rTL1A or media alone. (**D, E, F**) Sort-purified, CFSE-labeled CD4$^+$ T-cells from OT-II mice were cultured for 6 days with sort-purified MHCII$^+$

DCs, MHCII^{-} ILC3s or MHCII^{+} ILC3s, from either WT (D, E) or *Tnfrsf25*$^{flox/flox}$ *Rorc-cre* *RAG2*$^{-/-}$ (called DR3$^{\Delta ILC3}$) mice (F) with media alone, OVA peptide, or OVA peptide and rTL1A, as indicated. Proliferation index calculated by FlowJo is shown (E, F). One of four independent experiments is shown. (**G**) Sort- purified, CFSE-labeled CD4^{+} T-cells from OT-II transgenic mice were cultured for 6 days with sort-purified ILC3s in the presence of media alone, rTL1A, or with rTL1A plus co-stimulatory molecule blocking antibodies. All samples received OVA peptide in culture. One of two independent experiments is shown. (**H, I**) ILC3s sorted from *Tnfsf4*$^{flox/flox}$ or *Tnfsf4*$^{flox/flox}$ *Rorc-cre* (called OX40L$^{\Delta Rorc}$) (H) or *H2-Ab1*$^{flox/flox}$*Rorc-cre* (called MHCII $^{\Delta ILC3}$) (I) were stimulated with rTL1A and co-cultured with CFSE-labeled OTII CD4^{+} T cells. One of two independent experiments is shown. Data in B, E, F, G, H and I are mean ± SEM and were analyzed by Student's t-test (B) or one-way ANOVA (E, F, G, H, and I); ***P<0.001. See also Figure S5.

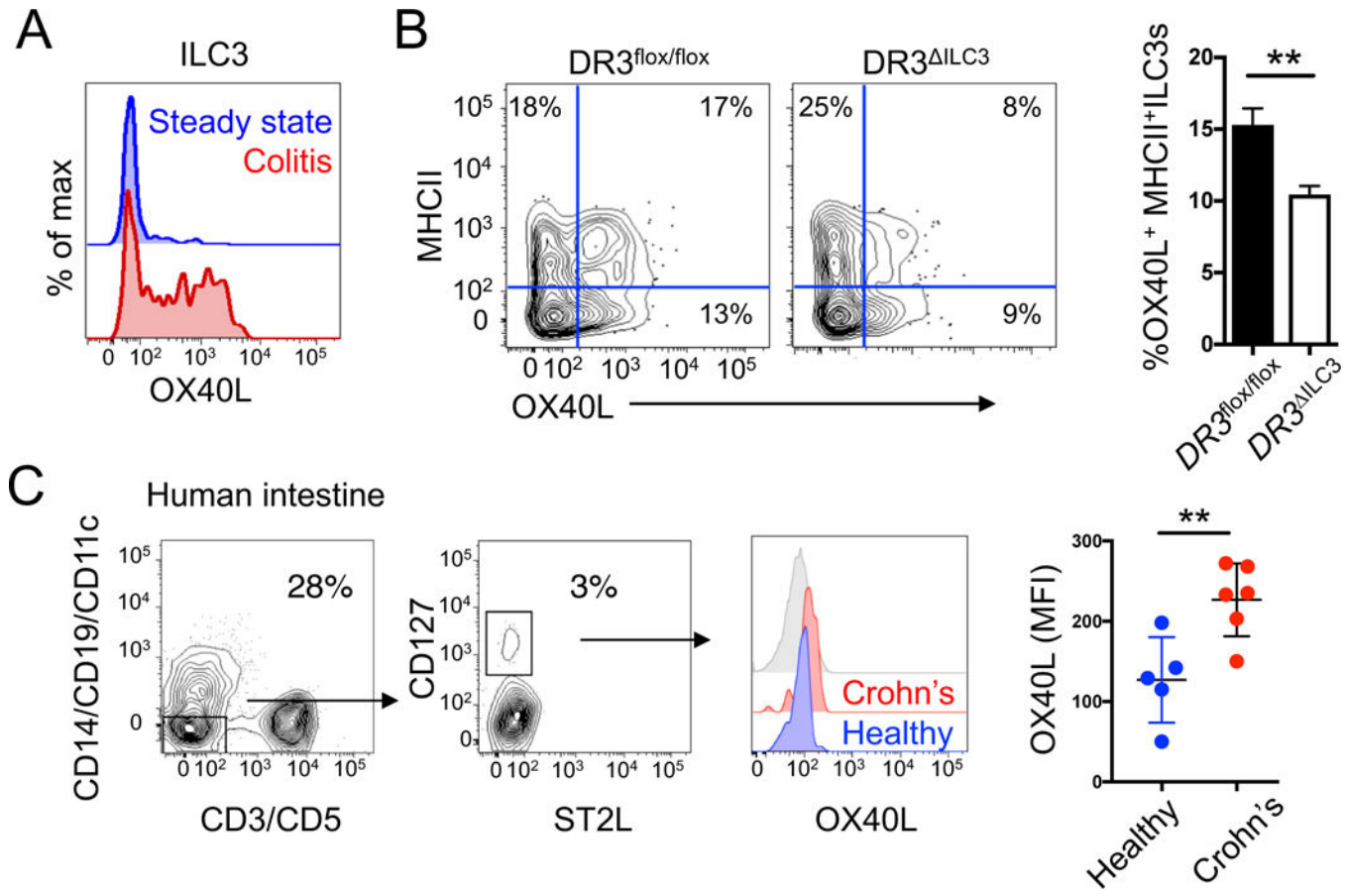

Fig. 6. TL1A induces ILC3 expression of OX40L during colitis *in vivo*.

(**A**) OX40L expression on Lin$^-$CD127$^+$ RORγt$^+$ ILC3s at the steady-state or following 2% DSS- induced colitis. (**B**) OX40L expression on Lin$^-$CD127$^+$ RORγt$^+$ ILC3s from *Tnfrsf25$^{flox/flox}$ RAG2$^{-/-}$* (called DR3$^{flox/flox}$) and *Tnfrsf25$^{flox/flox}$ Rorc-cre RAG2$^{-/-}$* (called DR3$^{\Delta ILC3}$) littermate mice following 2% DSS-induced colitis (N=4 mice/group). One of two independent experiments is shown. (**C**) Human OX40L on Lin$^-$CD127$^+$c-KIT$^+$ ILC3 from colonic biopsies of healthy patients or IBD patients with active inflammation (N=5–6 patients/group). Data in B and C are mean ± SEM and were analyzed by two-tailed Student's t-test; ** P<0.01. See also Figure S6.

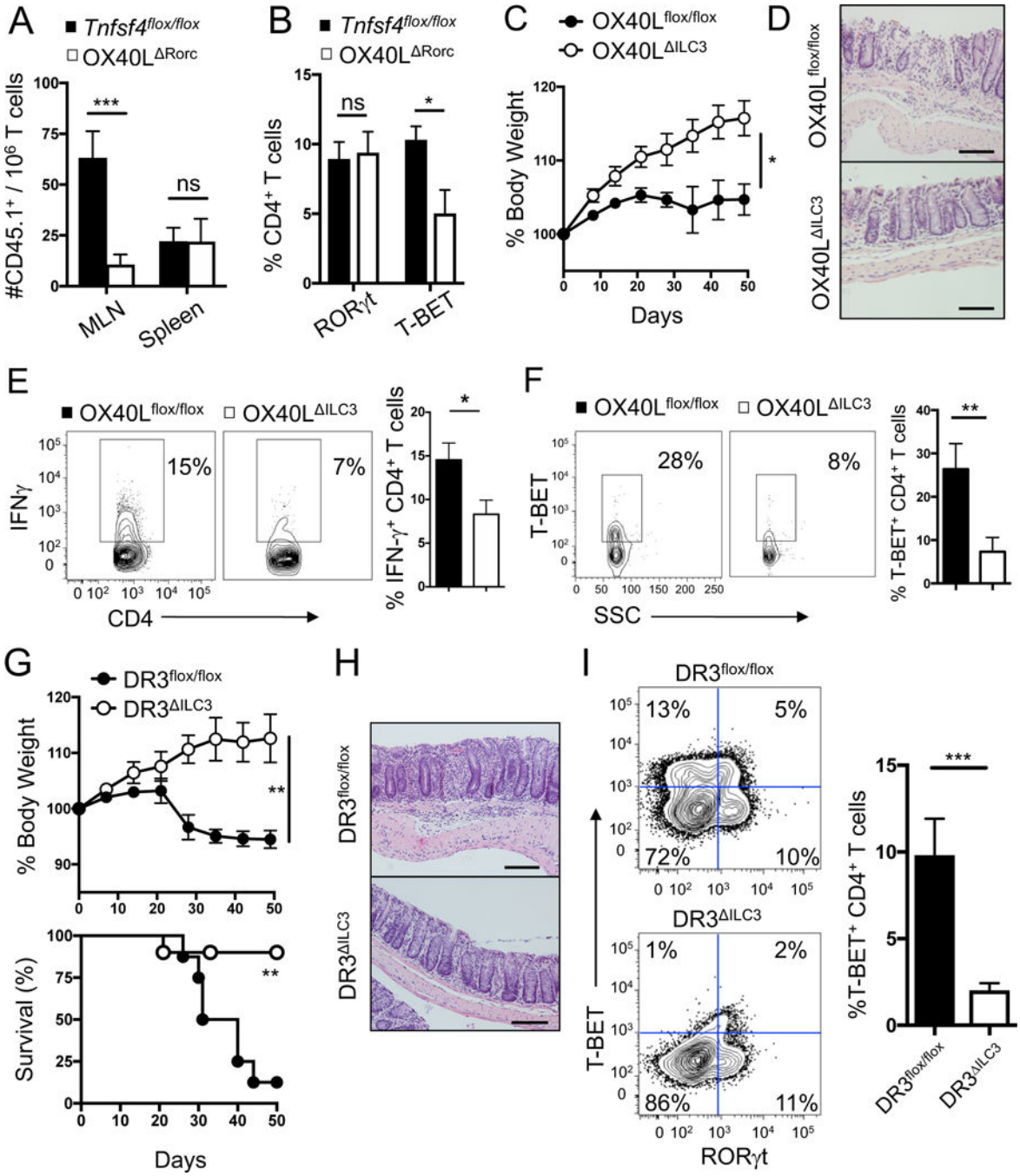

Fig. 7. ILC3 expression of OX40L regulates antigen-specific and T-BET$^+$ Th1 cell activation in T cell colitis.

(A) Transfer of naïve CD45.1$^+$ CD3$^+$CD4$^+$Vα2$^+$ OT-II T cells into CD45.2$^+$ *Tnfsf4*$^{flox/flox}$ or CD45.2$^+$ *Tnfsf4*$^{flox/flox}$ *Rorc-cre* (called OX40L$^{\Delta Rorc}$) mice treated with 2% DSS and ovalbumin for 5 days. Flow cytometric analysis of CD45.1 $^+$ CD3$^+$CD4$^+$Va2$^+$ OT-II T cells from compiled over two independent experiments (N=6–8 mice/group). (**B**) RORγt and T-BET in CD4$^+$ T cells from intestinal lamina propria of *Tnfsf4*$^{flox/flox}$ or OX40L$^{\Delta Rorc}$ littermate mice (N=4 mice/group). (**C, D**) Percent body weight (C) and representative

colonic histology (D) of *Tnfsf4*$^{flox/flox}$ *RAG2*$^{-/-}$ (called OX40L$^{flox/flox}$, N=8) and *Tnfsf4*$^{flox/flox}$ *Rorc-cre RAG2*$^{-/-}$ (called OX40L$^{\Delta ILC3}$, N=7) littermate mice following adoptive transfer of CD4^{+}CD45RB^{high} T cells to induce transfer T cell colitis. (**E, F**) Flow cytometric analysis of intracellular IFNγ (E) or intranuclear T-BET (F) in CD4^{+} T cells from OX40L$^{flox/flox}$ and OX40L$^{\Delta ILC3}$ littermate mice in (C). (**G, H**) *Tnfrsf25*$^{flox/flox}$ *RAG2*$^{-/-}$ (called DR3$^{flox/flox}$, N=6) and *Tnfrsf25*$^{flox/flox}$ *Rorc-cre RAG2*$^{-/-}$ (called DR3$^{\Delta ILC3}$, N=7) littermate mice following adoptive transfer of CD4^{+}CD45RB^{high} T cells to induce transfer T cell colitis. Body weights, percent survival (G) and representative colonic histology (H) from DR3$^{flox/flox}$ and DR3^{AILC3} littermate mice following adoptive transfer of CD4^{+}CD45RB^{high} T cells (scale bar: 100μm). (**I**) Flow cytometric analysis of T-BET induction in transferred T cells from DR3$^{flox/flox}$ and DR3$^{\Delta ILC3}$ littermate mice in (G) and (H). Data in A, B, E, F, and I are mean ± SEM and were analyzed by two-tailed Mann-Whitney test (A, B) or two-tailed Student's t-test (E,F,I). Data in C and G were analyzed by Log-rank (Mantel-Cox) test; * $P<0.05$, ** $P<0.01$, *** $P<0.001$. See also Figure S7.